Device to Alter Thermal Conductivity using Dielectrophoresis

A Major Qualifying Project

Submitted to the Faculty of

Worcester Polytechnic Institute

In partial fulfillment of the requirements for the

Degree of Bachelor of Science

In

Mechanical Engineering

By

____

Hudson Gasvoda

Date: 5/18/2020

Project Advisors:

____

Professor Ahmet C. Sabuncu

Abstract

Heat transfer is a vital part of temperature regulation in modern engineering systems. Temperature regulation for electronic devices prevents chips from overheating and deformation due to heat. Regulating the temperature is crucial to keep electronic systems operating at optimal efficiency. Increasing the heat transfer area to enhance the heat transfer rate is not possible for all small volume applications, and therefore, the medium through which heat transfer occurs must be altered by adding high thermally conductive particles to increase the heat transfer rate. In this study, we used dielectrophoresis to alter the thermal conductivity of 293 µm of gold colloidal solution. Polydimethylsiloxane chamber was used to house 3.96 microliters of gold suspension in between two metallic electrodes. In the experimental setup, one electrode was attached to a DC heater and the other was attached to a water/ice heat sink. Once energized, the electrodes create a nonlinear AC electric field between them. With the current active, the gold particles align themselves along the electric field lines. Using gold microparticles suspended in water at 1% volume ratio, RTDs recorded the temperature on each electrode to determine the change over time. We tested combinations of air, water, deionized water and gold suspension. The results note there is only a .061 °C difference in temperature when the particles align on electric field.

Table of Contents

List of Figures

1.0 Introduction

Thermal energy is involved in every process since energy is always lost due to heat. When the engine runs in a car, it heats up, like how a circuit board warms when an electrical current pass through it. With the heat energy being an unintentional byproduct of processes, it can directly influence the efficiency of the device. Too much thermal energy can cause part expansion, melting, increase in friction, and an imbalance in reactions. To limit the damage thermal energy can cause, it must be siphoned away. This can be done convectively, conductively, or via radiation. The predominant way is through conduction with heat sinks attached to a heated element and allowing thermal energy to flow away from the part.

Heat can cause electronic chip failure and many mechanical issues ranging from an increase in friction to a loss in efficiency since energy dedicated to work is now lost due to heat. To limit the effects heat has on a system, cooling methods act as a siphon, removing the heat allowing the system to run long periods of time without a significant loss in efficiency. With new electronic chip designs becoming smaller and more complex with higher heat fluxes, cooling systems need to remove heat more proficiently.

Since dielectrophoresis can align particles along a non-linear electric field to form micro chains spanning the electrode gap, these micro chains can aide in heat transfer and result in a higher thermal conductivity of the solution. In this experiment, dielectrophoresis was used to align a 1% gold colloid solution along non-linear electric field lines to create micro chains to increase the heat transfer rate of a system. To do this, the experiment was comprised of building a thermally isolated chamber capable of measuring the temperature of 2 electrodes, one that was connected to a heated element, and another that was connected to a cooling chamber. The electric field was formed by creating a circuit involving both electrodes and is completed by the solution in the gap. The temperatures of the 2 electrodes were recorded across 30 minutes. The data will be compared to other fluid mediums to determine if it offers a higher heat transfer rate. All thermal testing will be performed at

Figure 1 Burnt smooth motor-controller (Repair of burnt smooth motor ... - Data Recovery Ireland., n.d.)

Worcester Polytechnic Institute. The data collected over the course of this project will have further use in continued experimentation of colloidal fluids in heat transfer at Worcester Polytechnic Institute.

Functional Requirements and Design Constraints	
Cooling element must be constant temp	Optically clear chamber
Heating element must have constant power	Chamber must be non-conductive
Chamber material must have low thermal conductivity	Fluid between electrodes must be easily removeable
Electrodes cannot move during experimentation	RTDs must remain in contact with the RTDs
Cooling element must always remain in contact with electrode 2	Heating element must always remain in contact with electrode 1

2.0 Background

Temperature is a measurement of average kinetic energy of the particles present in a substance or object. The increase of temperature correlates directly to the increase in thermal energy. The increase of thermal energy is caused by molecules and atoms moving faster and colliding with each other. This increase of energy in an object can result in various problems. Higher heat results part deformities. These deformities can be localized at a certain point or can evenly spread across the entire body. The thermal energy causes additional pressure in contained gases and liquids. Additionally, the use of electronic chips generates heat since the inefficiencies of the electrical conduction components causes heat generation. Heat buildup can cause a dip in efficiency in devices since excessive heat lowers the resistance, thereby raising the current. To minimize these disadvantages, thermal regulation devices were created to keep electronics operating at long times in a window of workable temperatures.

2.1 Thermal Regulation Devices

Difference regulations devices function differently but have the same end goal. The operating differences can have different devices work better under different conditions. Additionally, a thermal management device may work better than others depending on the system it is involved in.

For electronics, the most commonly used thermal management device is heat sinks. Heat sinks are designed to be in contact with an electronic components hot surface. There are passive, semi-active, and active heat sinks. Passive designs use natural convection or when the heat dissipation is not dependent on the air flow supply. Semi-active ones leverage the fluid flow through preexisting fans to produce impingement. An active heat sink has a fan designated for its own use which is often built into the design of the heat sink. However, the reliability of this design is directly correlated to its moving parts, namely the fan.

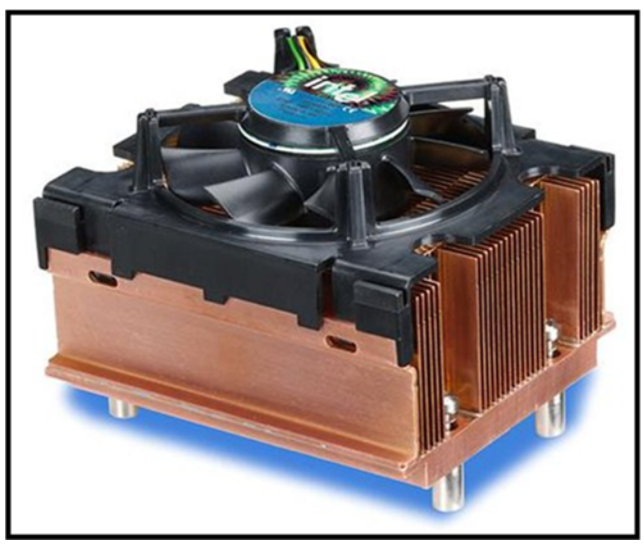

Figure 2 Active heat sink with built in fan (Newegg, n.d.)

Depending on the thermal density of the system, there are many different heat sinks designs to choose from. The stamping technique, which has copper or aluminum sheets stamped into the desired shape. While it is a low-cost process, it solves low density thermal problems. Heat sinks can be cast out of high-density aluminum and copper to allow for maximum performance and can make custom shapes but are more expensive. Extrusion can form complex 2-D shapes that increase the performance, but the designs are limited by the fin's height-to-gap ratio, the minimum fin thickness-to-height, and the maximum base to fin thickness. With bonded and fabricated fins, a thermally conductive epoxy bonds the planar fins to the grooved extrusion plate. By bonding, a greater fin height-to-gap aspect ratio can be achieved along with the cooling capacity without increasing the volume. However, a disadvantage is the usage of the thermal epoxy, which has a lower thermal conductivity thereby increasing the thermal resistance. The final option is folded fins which has sheet metal folded into fins and attached to a base plate or the heated element via epoxy or brazing. Due to the availability and fin efficiency, the folded fin design is not suitable for high profile heat sinks but is a suitable option when extrusion or bonded fins are not usable (San Jose State Mech Eng Department. (n.d.)).

With the contact to the component, a thin thermal material is put in-between the surfaces that can also affect the transfer rate by closing the air gaps between the heat sink and the component. Factors that determine a heat sinks effectiveness are air velocity, choice of material, protrusion (fin) design, and surface treatment. To overcome a low air velocity, fans are usually used in conjunction with a heat sink (Lee, 1995).

Another way to conduct heat transfer is through heat pipes. A heat pipe is a heat transfer device that uses phase transition and thermal conductivity to transfer siphon heat from a source. Heated pipes work as an evaporation condensation two-phase device that transports large amounts of heat between a cold and hot interface with a coolant. Typically, a heated pipe consists of a sealed hollow tube and a wick to return the working fluid to the condenser from the evaporator. The pipe contains a saturated liquid and a vapor of a working fluid. A common heat pipe setup for electronics in space is aluminum and ammonia (Advance Cooling Technologies, n.d.).

A Peltier Cooling Plate uses the Peltier effect to make a heat flux between the junction of two different conductors. An example of the Peltier effect is a thermocouple. In the circuit of the thermocouple, an electric current passes through the couple having heat generation at one junction and absorbed at the other. This is the Peltier effect, which mathematically describes the heat transfer rate, $\dot{Q}$, as:

$$\dot{Q} = \frac{(\Pi_A - \Pi_B)}{I} \quad (1)$$

where Π_A and Π_B are the Peltier coefficients of conductors A and B with I being the electrical current between A and B. Many of these junctions can be created in series to create the desired cooling required. While it has no moving parts, its efficiency is low, so it is generally used for electronic devices that need to operate at a temperature below ambient air (FerroTec, n.d.).

By using the continual flow of vortices created by alternating blasts and suctions of air in an opening, synthetic jet air cooling produces a net mass flux of zero while directing the airflow to precise locations of hotspots. The jets are formed from the working fluid of the system to produce a net momentum without a net mass injection (Jones & Rodgers, 2014). Since they have no moving parts, the maintenance is minimal and show higher heat transfer coefficients than typical fan flow (Mahalingam, 2019).

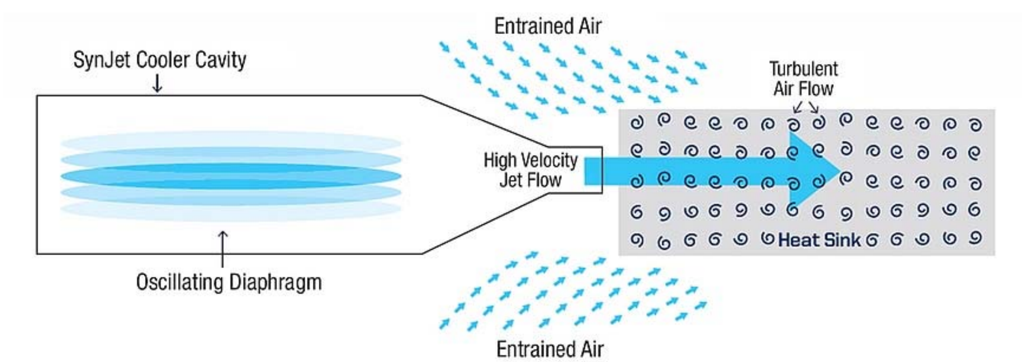

Figure 3 Synthetic Jet Air Cooling diagram. (Jones & Rodgers, 2014)

Finally, an electrostatic fluid accelerator (EFA) which pumps a fluid without any moving parts. By creating an electric field to propel charged fluid molecules and a way to recapture and neutralize the charged particles, EFA is able to be a viable cooling process for micro-electronics (Wang, Jewell-Larsen, & Mamishev, 2013). The heat transfer performance of the EFAs is comparable with convectional rotary fans, but the advantage of EFAs is the small volume and lower acoustic level.

2.2 Dielectrophoresis

When neutral particles move towards a position of maximum field strength in a nonuniform electric field, the phenomena is known as dielectrophoresis (DEP) (Pethig, 2017). DEP is different from the electrophoresis, which has motion of particles in a spatially uniform electric field. Cataphoresis is when positively charged particles undergo electrophoresis, while the motion of negatively charged particles is called anaphoresis (Pethig, 2017). The non-uniform electric field is formed by applying an AC current between two electrodes that can vary in design. All particles exhibit dielectrophoretic activity under the presence of a non-uniform electric field. The strength of the force is heavily correlated to the medium and the electrical properties, shape and sizes of the particles, as well as the frequency of the field (Dukhin, Ulberg, Gruzina, & Karamushka, 2014). However, the electrophoretic force on a charge is equal to the electric field multiplied by the charge of the particle, and if there is no charge then the force is 0. If a dipole's net charge is zero, then it will experience a torque, but not a translational force. In an inhomogeneous field, there is also a translational force acting upon the dipole (GRIMNES, 2017). The force on a particle ***F*** can be calculated in field gradient, $\nabla \boldsymbol{E}$ by (Pethig, 2017):

$$< F >= 2\pi r^3 \varepsilon_m Re\{\frac{\varepsilon_p^* - \varepsilon_m^*}{\varepsilon_p^* + 2\varepsilon_m^*}\} \nabla |E_{rms}|^2 \qquad (2)$$

where $\varepsilon_p^* = \varepsilon_p - \frac{j\sigma_p}{\omega}$; $\varepsilon_m^* = \varepsilon_m - \frac{j\sigma_m}{\omega}$. In equation (2), ***r*** is the radius of the particles, ***Re*** represents the real function of the Clausius-Mossotti Factor, the fluid medium complex dielectric characteristic is $\boldsymbol{\varepsilon_m^*}$ while the particles is expressed as $\boldsymbol{\varepsilon_p^*}$. $\nabla|\boldsymbol{E_{rms}}|^2$ is the gradient of the electric field squared to quantify the non-uniformity of the electric field. The Clausius-Mossotti Factor expresses the dielectric constant in terms of the materials constituent atoms/molecules, or in terms of atomic polarizability, or as a homogenous mixture of the two (Belle, Rip, Böttcher, & Bordewijk, 1973). Through this force, there is both positive DEP and negative DEP. Positive DEP groups particles nearest to the electrodes while negative DEP groups particles between the two based upon the force applied to the particle (Pamme, 2008).

DEP has a variety of uses ranging in different fields from biomedical applications to nanowire formations. For biomedical uses, DEP has been integrated into a lab-on-a-chip system to create point-of-care (POC) systems. These POC systems are used for early detection and diagnosis of various cancer types, infectious diseases, blood cell analysis, and stem cell therapy. However, since the field is relatively young, DEP is being used for a wide variety of biological applications ranging from particle separation, manipulation, to enrichment for diagnosis (Demircan, Özgür, & Külah, 2013). For particle separation, DEP can separate based on dielectric properties, by particle size. Additionally, the electrode design can aide in particle separation as well, offering microfluidic channels to filter different particles.

One of the major breakthroughs in the field was the separation of cancer cells from other blood cells in continuous flow via DEP field-flow-fractionation (FFF) (Separation of cancerous cells from other blood cells in continuous-flow by dielectrophoresis field-flow-fractionation). FFF is a separation technique applied to fluid suspensions that is pumped through a long and narrow channel to cause particle separation through a separation field (Gascoyne, Wang, Huang, & Becker, 1997). In this study, MDA-231 human breast cancer cells were removed from blood at a separation rate at least 10^3 cells per second. This separation technique did not harm cell viability. It is noted that MDA-231 cells have a specific capacitance of 26 mF/m^2 while T-lymphocytes are only at 11 mF/m^2. The combination of the DEP and the flow focusing allows the cells to be separated based on particle dielectric properties.

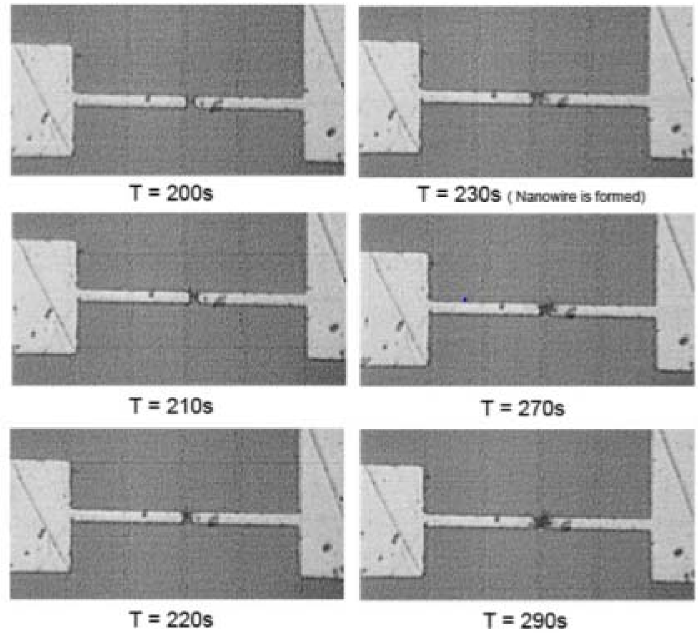

Figure 4 Results of PCF under positive DEP force. (Leung, Li, & Li, 2008)

Not only is DEP used for biological purposes, it can also be used for chain formation. Chain formation is best described as particles aligning along the electric field, forming a “chain” between the electrodes. The use of gold nanoparticles has been extensively studied for its potential applications in nanomedicine, and nano-photonics, and wiring for nanodevices ((Leung, Li, & Li, 2008). Additionally, with the advance of nanowire fabrication techniques has allowed the formation of a nanowire to change. For example, the vapor-liquid-solid (VLS) synthesis is a 1-D mechanism for crystal growth. In the method, an Au-Si droplet is deposited on a wafer surface and grows a silicon whisker crystal through a catalytic liquid alloy phase of gold and silicon that rapidly absorbs a vapor up to supersaturated levels, allowing the whisker growth to proceed from the liquid-solid interface (Wagner & Ellis, 1964). One downside of VLS is that is limits the uses of the nanowire due to a minimum wire size, so the usage of the DEP technique has risen (Ozturk, Flanders, Grischkowsky, & Mishima, 2007). Through DEP, the conductive particles are aligned along the field gradient towards the tips of the electrodes. To remove the chain, the electrode is pulled away from the colloidal liquid and drags particles to form a chain (Rozynek, Han, Dutka, Garstecki, Józefczak, & Luijten, 2017).

2.3 Evolving Electronics and the Heat Problem

With electronic devices dominating today's economic market, companies struggle to make smaller, better, faster electronic chips for their devices. However, the efficiency of these devices is related to their temperature. In order to remain at low temperatures to function optimally, the cooling systems must evolve to maintain operational stability. at a commensurate rate. With a growing number of electronic chips failing due to heat, efforts to improve reliability and durability of electronic computers is as important as improving their speed and storage capacities (Chu, 2004).

With the trend of higher circuit density and reductions of circuit delay, the increase of heat flux is rising at a challenging rate. The challenge facing thermal engineering is to limit chip operating temperatures with every new generation of chip design. As the size of semiconductors reduces, the leakage power dissipation can become even greater than the active device power dissipation. Additionally, the cost of running the cooling systems is increasing with each chip generation so companies are looking for low-cost and more effective options. In order to neutralize the high heat flux from chip's circuits, there is need for the development of low cost and high thermally conductive materials such as thermal pastes and spreaders (Chu, 2004). Advanced techniques in cooling like heat pipes and vapor chambers are already in use. Further advances in these technologies and in thermoelectric cooling, direct liquid cooling, high-performance air-cooled heat sinks, and air movers are also needed to properly maintain chips at an operable temperature.

3.0 Materials and Methods

3.1 Thermal Behavior of Suspensions

The thermal conductivity of a fluid medium is altered with the addition of a particle in suspension. If the transport properties are neglected, then the system becomes a static inhomogeneous dispersion of particles in a fluid medium. Maxwell developed a theory for thermal conductivity of the colloidal solution which operates on the assumptions that all particles are spherical and unmoving with a temperature profile that is continuous (Maxwell, 1954). Maxwell's models the relation of the thermal conductivities of the suspended particles and the fluid by

$$\frac{k}{k_f} = \frac{k_p + 2k_f + 2\emptyset(k_p - k_f)}{k_p + 2k_f - \emptyset(k_p - k_f)} \qquad (3)$$

with $\boldsymbol{\emptyset}$ representing the volume fraction of 0.01 and $\boldsymbol{k_f}$ is the thermal conductivity of the fluid which is 0.555 for deionized (DI) water at 20 °C. The gold particles have a conductivity of $\boldsymbol{k_p}$ of 314 W/mK. Through the Maxwell model, the overall thermal conductivity of the colloidal solution is 0.572.

3.1 Device Fabrication

To be able to see if the colloidal medium has any influence on heat transfer, building a chamber that can house the heating element, cooling element, electrodes, and the fluid medium is needed. The chamber should also be optically clear to be able to see if there is leakage during the experimental process. Additionally, the

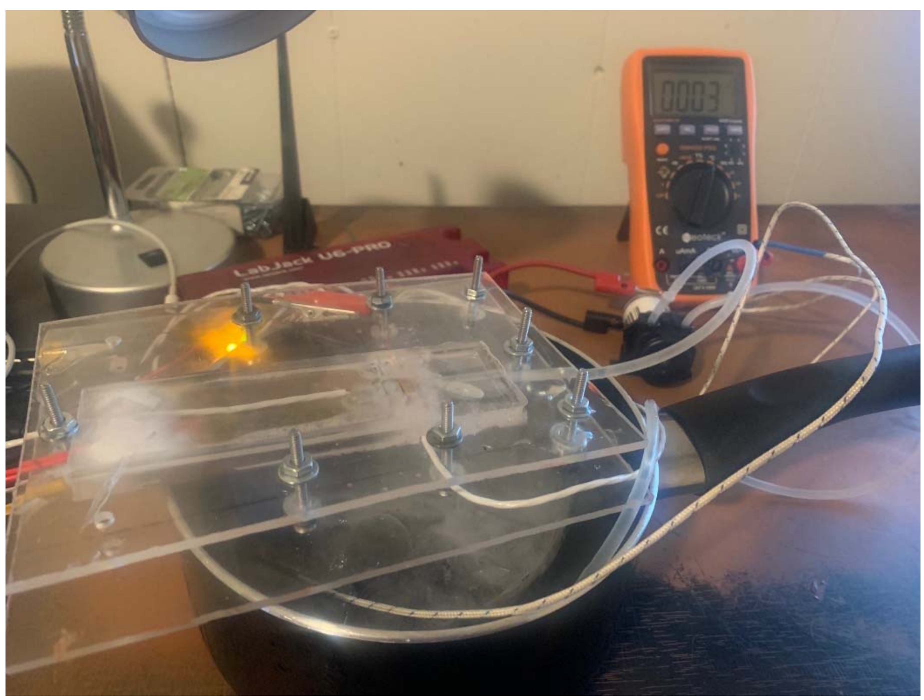

Figure 5 Experimental Device with ice bath, pump, multimeter, data acquisition box, and acrylic plates

chamber should have a low thermal conductivity to limit the heat transfer to the outside environment.

3.1.1 Cooling Chamber Design

For the chamber to have a 1-D transient heat profile, the direction of heat flow must be dependent on only one axis. The easiest way to do this is to have heat flow from conduction. By having one side heated and the opposite side cooled, the heat will dominantly flow in the direction of the greatest temperature gradient. To build the chamber, one side has a heating element, a stick-on heater from Omega engineering. The heater allows control over the power input into the system, minimizing discrepancies in thermal conductivity calculations of the fluid mediums. On the other side there is a cooling element, or in this case an ice bath. The ice bath siphons heat from the rest of the system, keeping the direction of heat flow constant.

Along with the chamber needing a directional heat flow, the chamber material must also be optically clear enough to see through while maintaining a low thermal conductivity. In this experiment, PDMS Sylgard 184 is a silicon elastomer kit that cures clear and has a thermal conductivity of 0.27 W/mK (Sylgard, n.d.).

3.1.2 Mold Fabrication

To create the chamber, there needs to be a mold to pour for the PDMS to cure in. The mold is modeled by taking the chamber design in AutoCAD and creating a negative into a solid Aluminum stock piece. For the mold, it was divided into a top and bottom piece to allow simple machining. The molds were machined at Worcester Polytechnic Institute’s Machine Shop using a Haas CNC Mini-Mill. Once the molds were created, the Sylgard 184 kit was mixed at a 10:1 mass ratio of base to hardening agent. With the mold filled with PDMS, they were placed in a vacuum chamber to remove the bubbles to maintain optical clearness. After 30 hours of curing time, the PDMS chamber pieces were removed from the aluminum molds.

3.1.3 Electrode Design

The second piece of fabrication is the electrodes. The electrodes are modeled in AutoCAD and then sent to Advanced Manufacturing Techniques Inc. to be machined out of to be created by means of electrical discharge machining (EDM) of Stainless Steel 316SS. In both designs, there are some radial cutoffs that reflect the tool radius that are shown when two sides come together to form a corner.

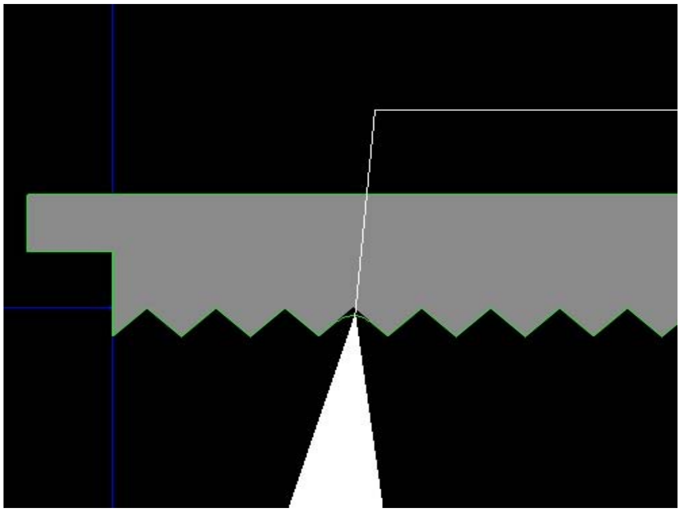

Figure 6 Radii of the EDM discharge

To create the experiment chamber, a mold to pour the PDMS is made. By designing the top and bottom layer of chamber separate, each can be used as a negative to make the mold. These molds are manufactured using an Aluminum 6061 flat bar stock piece and a 3-axis CNC HAAS mini-mill. Radii are imposed on the inner right angles of the mold due to the tooling radii. The molds are then filled with 10:1 mass mixture of Sylgard 184 Silicone Elastomer. To prevent bubbles formation, a vacuum chamber houses the mold after the pouring. The PDMS can cure for 24 hours in the vacuum chamber before it is removed from the mold. To increase the firmness of the PDMS, additional curing agent can be added.

3.1.4 Electroplating

In order to increase the thermal conductivity of the electrodes, they were electroplated in 24K gold. The process for the electroplating requires soap, DI water, an acid dip solution, electrocleaning solution, and activation solution, and a gold plating solution. Between each process, there is a DI water dip of the electrodes to remove any residual solution before the next step in the plating. To start the electroplating process, the electrodes must first be placed in a soap and water solution and scrubbed with a soft bristle brush

Figure 7 Electroplated stainless-steel electrode

to remove all the surface contaminants. Next, the electrodes undergo an electrocleaning in NaOH 40 g/L + Na2CO3 25 g/L solution at 0.1 A/cm^2 at 6 V for 2 minutes. After that, there is an acid dip of Midas Acid Dip at a concentration of 0.1669 g/mL and it is set to 1.5 minutes. Succeeding the acid dip is another round of the electrocleaning. Next, there is a Surface Prep Solution, to remove the oxide layer on top of the stainless steel to make it ready for an ionic metal. Subsequently, another electrocleaning with the same properties is run. Following the third electrocleaning, the electrodes are immersed in a gold solution. The current of the gold plating is 5mA/inch^2 of surface area which converts to .001 mA/mm^2. The total current is run at .079 mA and 3 V. They are attached to the anode since the electroplating process bonds the extra surfaces electrons with an anode. The anode is considered to be the positively charged gold particles in the solution, and when bonded, produces a non-ionic film of gold (Lewis, 2019).

3.2 Assembly

To build the setup, electrode 2 is connected to the RTDs via a thin film of cyanoacrylate. The thermal conductivity of the super glue can be considered negligible due to the thinness of the super glue layer. Once the RTD is connected to electrode 2, the electrodes are fitted into PDMS grooves built to align the them facing each other. A notch is cut into the PDMS under electrode 2 so the RTD wire can feed underneath and out the side. Under the side wall is a groove attached to the notch to make room for the RTD wire so it cannot cause a bend in the setup. Two cutouts in the bottom side walls around the water chamber allow water to flow in and out of the chamber, constantly feeding in cold water.

Figure 8 Copper plate with stick on heater and RTD

The stick-on heater and an RTD is stuck to a piece of copper sheeting to force the directional flow of heating. The copper sheet is connected to electrode 1 via physical touch and thermal paste that conducts heat at 5W/mK. The heater is powered via a BK Precision 1550 power supply a DC output of 16.0 V and 0.17 amps.

Creating a seal between the top and bottom layer of PDMS allows the contents inside to be thermally isolated from the outer environment. To make this seal, 2 pieces of acrylic an acrylic sheet are placed on the top and the bottom of the chamber and bolted together to put pressure on both PDMS pieces to seal them together.

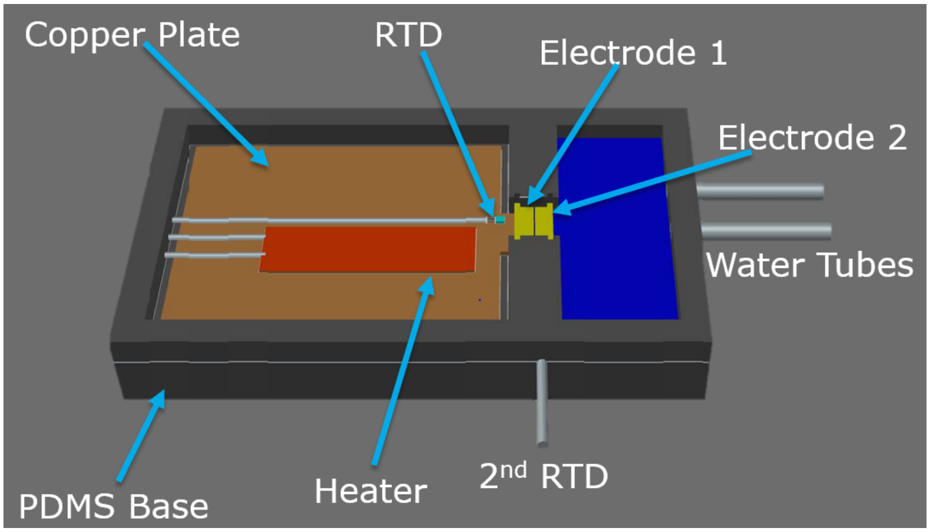

Figure 9 Bottom chamber with all interior pieces

Finally, an external ice bath is used with a DC 12 V pump to circulate the water between the ice bath and the PDMS water chamber. To create a 1-D thermal flow, the water is kept at a constant cold temperature via ice to direct the heat flow from the heater.

Figure 10 12 VDC pump

3.3 Thermal Measurements

To acquire the temperatures at the electrodes, resistance temperature devices (RTDs) are connected to Electrode 2 and the copper plate near Electrode 1. These RTDs are wired to a LabJack U6-Pro data acquisition box. The U6-Pro has a constant current output connection, so that is used with the RTDs wired in series to create one circuit with one constant current. With the constant current, the voltage is changing in direct relation to the resistance of the RTD. In order to see the voltages between the electrodes, they were wired in series with inputs in front and behind each electrode. The overall voltage drop across the wires is considered 0V. To find the resistance of the RTDs using the equation

$$R_{RTD} = (V_1 - V_2)/I \quad (4)$$

where V_1 is the voltage before the RTD and V_2 is the voltage after the RTD. I is the constant current of the LabJack output which was 197 µA. After finding the resistance of the RTD, the temperature can then be found via

$$T = \frac{\frac{R_{RTD}}{R_0} - 1}{A} \tag{5}$$

with R_0 equaling the resistance of the RTD when the temperature is registered at 0 °C. A represents the temperature coefficient which is .00385 for a platinum 100 Ω resistor.

3.4 Setup

To gather data, the proper fluid medium must be pipetted in-between the electrodes. Then the top piece of PDMS can be placed on top of the bottom piece. Once the ice bath tubing is connected to the pump, ice bath, and water chamber, then the acrylic sheets can be screwed together using nuts and bolts. To create an adequate seal, the bolts must be tightened a full 2 turns past snug. Once this is done, the ice bath must be filled with ice and water. The pump, plugged into a 9 VDC plugin, can be turned on to start cycling the cold water into the chamber to cool electrode 2. After an adequate time has passed, the DC power supply of the heater is turned on as well as the LabJack acquisition software, LJLogUD.

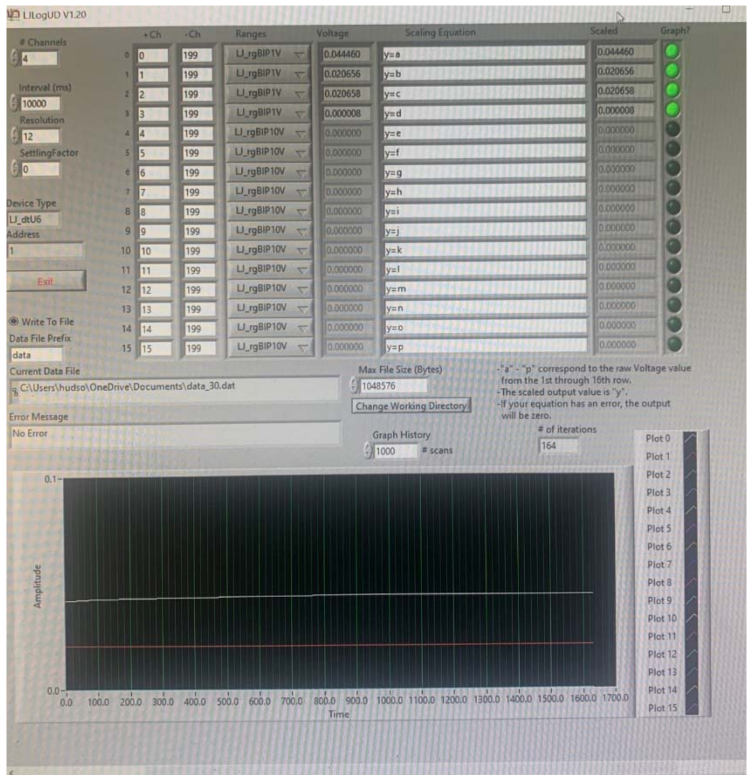

Figure 11 LabJack LJLogUD

LJLogUD is LabJack's software built in LabView. In it, there is a selection of the number of analog inputs, which is 4. The time interval between each data recording was set at 1000 ms with a resolution factor of 12. The settling factor was kept at 0. For the ranges of the input channels, it was changed to LJ_rgBIP1V due to the low voltage of the circuit.

3.4.1 DEP Setup

For the setup of the AC current, there are 2 small wires that are connected to the electrodes via silver epoxy. The silver epoxy allows an electrical current to pass through the wires to the electrodes to have a non-linear AC current in the fluid medium between the electrodes. The AC current is a sine wave created by a signal generator that has a phase shift of 180°. The frequency is in 0.1-6 MHz range and the voltage varies between 1-4 V range. To find the gap thickness between the electrodes, a test of the resistance of DI water is used. The resistance of DI water at 25 °C is 18.2 MΩ/cm (Myron L Company, n.d.). To measure the resistance of the fluid medium, attach a resistance multimeter to the wires attached to the electrodes. With a current generated from a multimeter, the resistance can be recorded.

4.0 Results and Discussion

Using the chamber, the temperatures at the electrodes were measured using RTDs to find the temperature differential across the microfluidic chamber. We started measurements with an empty chamber and chamber filled with deionized water and gold suspension. We expect that the temperature differential will change as the gold microparticles align in a non-linear AC field. Once the transient temperatures were plotted, the thermal conductivities were calculated to determine if the alignment due to dielectrophoresis showed an additional increase beyond the increase from the gold particles to DI water. The below sections show the process to obtain the thermal conductivity from the measured temperatures.

4.1 Electrode Gap

Table 1 Electrical Resistance of DI water and the gold colloid solution

Water (MΩ)	**0.512**	**0.518**	**0.572**	**0.525**	**0.539**	**0.5332**
Gold Solution (kΩ)	158.8	162.2	167.3	169.4	154.7	162.48

The gap between the electrodes was calculated measuring the average electrical resistance of DI water using a multimeter. With a set resistance of 18.2 MΩ/cm, we could estimate the electrode gap distance T_e using equation (6)

$$T_e = \frac{R_w}{R_{w/cm}} \tag{6}$$

where Rw is the measured resistance and Rw/cm is the resistance of DI water per centimeter. Thus, the gap was calculated to be around 293 µm. Table 1 also has the resistance of the gold colloid solution showing an average drop in electrical resistance of 69.53% compared to the DI water.

4.2 Thermal Conductivity of the Electrodes

The electrodes are made of stainless steel electroplated with a thin layer of gold. Since this creates a heterogenous material, we needed an effective thermal conductivity for this material. The following technique was used to calculate the effective thermal conductivity. The total thermal resistance is calculated using equation (7).

$$R_{TTC} = R_1 + R_2 + R_3 + R_4 + R_5 + R_6 + R_7 \tag{7}$$

with $\boldsymbol{R_1}$ thru $\boldsymbol{R_6}$ representing the thermal conductivity of the gold electroplated layers, one on each face of the electrode and R_7 representing the stainless steel 316SS core. $\boldsymbol{R_\#}$ is also expressed by

$$R_{\#} = \frac{L_{\#}}{k_{\#}A_{\#}} \tag{8}$$

where $\boldsymbol{L_{\#}}$ is the length the thermal energy transfers across, $\boldsymbol{k_{\#}}$ is the thermal conductivity of the material, and $\boldsymbol{A_{\#}}$ is the cross-sectional area. With gold having a thermal conductivity of 314 W/mK and assuming a thickness of the gold electroplated layer of 1 µm, the thermal conductivity of the gold and the stainless steel is calculated by taking the thermal resistance of each layer of gold and the stainless steel, and adding them to get the total thermal resistance of the electrode.

Table 2 Thermal Resistance of the electroplated electrode

	Left Side	**Right Side**	**Top**	**Bottom**	**Front**	**Back**	**Stainless Steel**
Length (m)	3 E-3	3 E-3	3 E-3	3 E-3	1 E-6	1 E-6	3E-3
Cross-Sectional Area (m^2)	1.5E-9	1.5E-9	9E-9	9E-9	1.35E-5	1.35E-5	1.35E-5
Resistance (K/W)	6369.43	6369.43	1061.57	1061.57	2.36E-4	2.36E-4	13.63

The total thermal resistance of the electrode is calculated to be R_{TTC} = 13.6327 K/W. Taking R_{TTC} to find the total thermal conductivity by

$$R_{TTC} = \frac{L_t}{k_t * A_t} \tag{9}$$

with $\boldsymbol{L_t}$ being the total length of the electrode, $\boldsymbol{k_t}$ being the total thermal conductivity, and $\boldsymbol{A_t}$ being the total cross sectional area. The thermal conductivity can now be calculated for the e; of the electrodes is 16.275 W/mK. This thermal conductivity is representing the electrode when it is stainless steel electroplated with gold.

The thermal conductivity of the electrodes allows the temperature profile across length of them to be considered constant. Additionally, by comparing the thermal conductivity of the electrodes and the fluids shows that the electrodes conductively transfer heat 28.45 more efficiently than the 1% by volume water and gold mixture. Because of this, the temperature difference across the electrodes can be considered negligible for calculations regarding the colloidal solution.

Table 3 Thermal Conductivities of the electrodes and fluids

Electrodes 1,2	Air	Water	Water + Gold
16.275	.02587	0.555	.572

4.3 Temperature Difference Between Electrodes

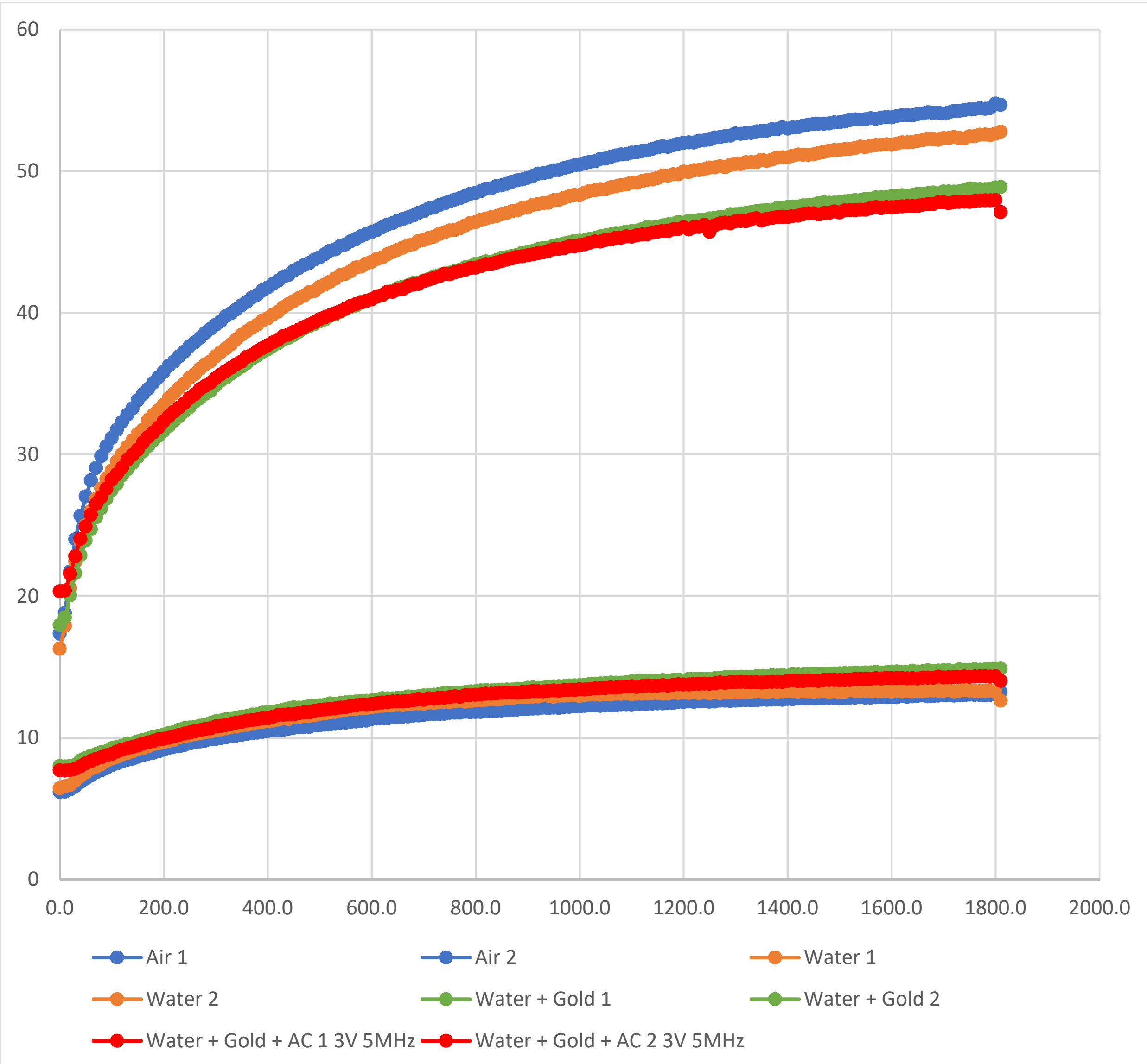

Figure 12 Comparison of the average temperatures with different mediums

By taking the temperatures from the graph at 1800 s, the thermal conductivities can be calculated and compared to the theoretical values. To find the experimental values, the equation

$$q = \frac{k}{L} * A * \Delta T \tag{10}$$

with ***q*** equaling power in, ***k*** is the thermal conductivity, ***L*** is the thickness, ***A*** is the cross-sectional area, and ***ΔT*** is the temperature difference. By re-arranging the equation to get

$$k = \frac{q * L}{A * \Delta T} \tag{11}$$

The thermal conductivity can now be calculated.

Table 4 Thermal conductivity of the fluids at time t = 1800s

	Length	Cross-Sectional Area	Power in (W)	ΔT (K)	Thermal Conductivity (W/mK)
Air	293E-6	1.35201E-5	3.34	41.443	1.747
Water	293E-6	1.35201E-5	3.34	39.527	1.831
Water + Gold	293E-6	1.35201E-5	3.34	33.965	2.131
Water + Gold 3V, 5 MHz AC	293E-6	1.35201E-5	3.34	33.605	2.154
Water + Gold 1.5V, 5 MHz AC	293E-6	1.35201E-5	3.34	33.144	2.184
Water + Gold 2V, 5 MHz AC	293E-6	1.35201E-5	3.34	32.472	2.229
Water + Gold 4V, 5 MHz AC	293E-6	1.35201E-5	3.34	31.352	2.309
Water + Gold 3V, .1 MHz AC	293E-6	1.35201E-5	3.34	31.524	2.296
Water + Gold 3V, .5 MHz AC	293E-6	1.35201E-5	3.34	37.583	1.926
Water + Gold 3V, 1 MHz AC	293E-6	1.35201E-5	3.34	33.816	2.140
Water + Gold 3V, 3 MHz AC	293E-6	1.35201E-5	3.34	33.065	2.189
Water + Gold 3V, 6 MHz AC	293E-6	1.35201E-5	3.34	32.502	2.227

Operating under the assumption that the electrodes have no drop of temperature across its length, the thermal conductivity of the solutions in the gap is listed above in the table. Reasons for the conductivity being higher than the previous reported values for the colloidal solution could be due to the gold settling on the bottom of the chamber, creating a thin film of gold for the thermal energy to transfer through.

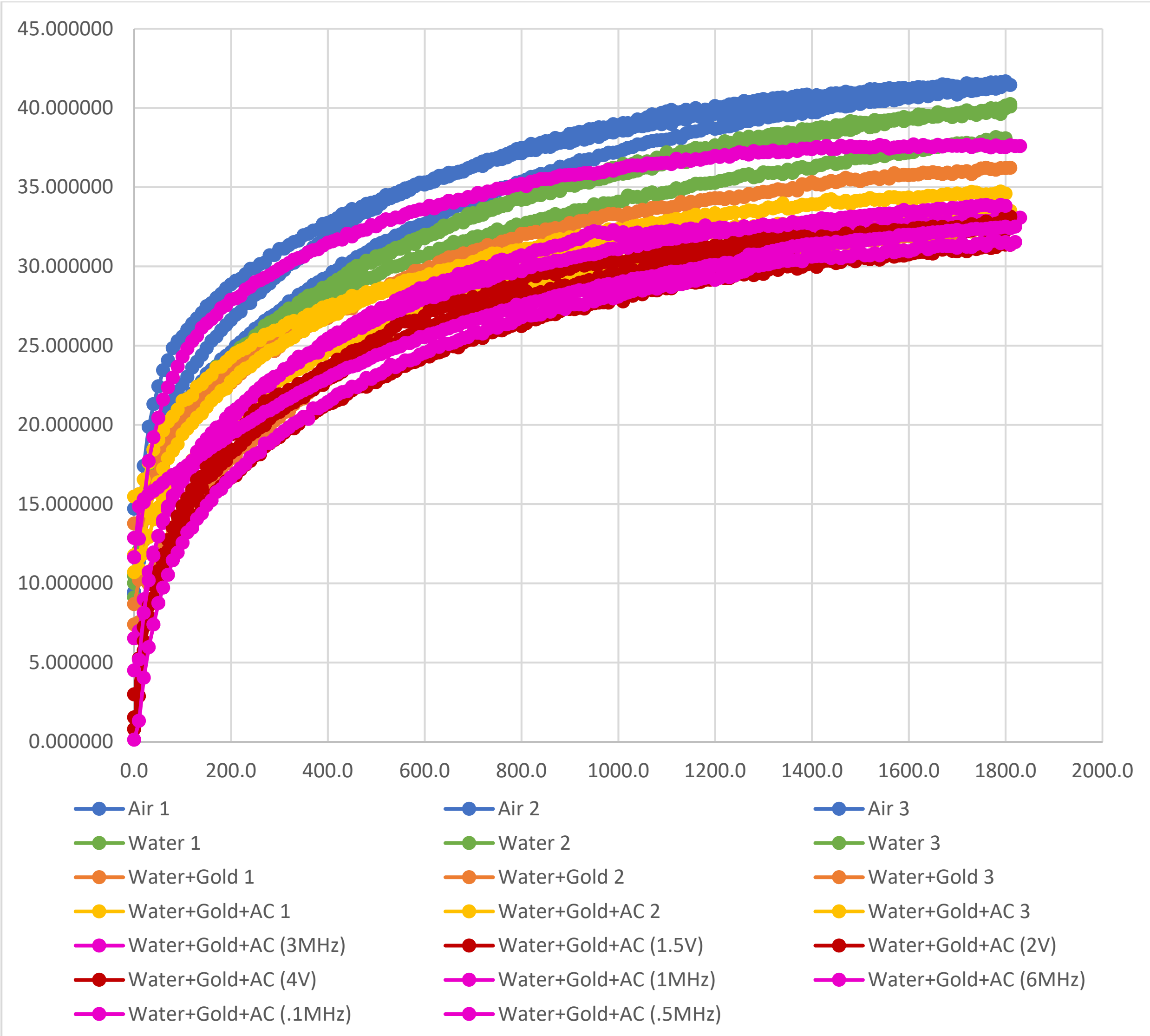

Figure 13 Electrode temperature differences

5.0 Conclusion

The addition of gold particles to the water improves the thermal conductivity over water by .017 W/mK. The temperature difference between the two mediums is 0.061 °C while the difference between water and air is 2.144 °C. While the addition of the gold colloid does increase the thermal conductivity, the addition of the AC current to align the gold particles does not have an experimental significant difference in temperature.

For the experiment, there are a variety of improvements to be made. By designing a way to pump in fluid between the electrodes, the chamber could become 1 solid piece and not require the acrylic to seal it. The top and bottom PDMS pieces could then be connected by a thin layer of PDMS to act like a glue, resulting in a completed chamber with no need for the additional pressure. Another way to connect the two pieces is through plasma bonding. Also, to gain a more accurate representation of the temperature change of the system, having a cooling system that is easier to maintain at a constant temperature is needed to limit factors changing the temperatures. Along with these changes, using a different fluid with a higher boiling temperature than deionized water will further highlight the temperature difference between the electrodes since more thermal energy can be used in the system. Since the SA1-RTDs have an accuracy of ± 0.15°C/0.06 Ω, using a more accurate and precise temperature measurement device can lead to better data. And finally, fabricating larger electrodes to increase the surface area of heat transfer can aide highlighting the thermal conductivity differences. With the addition of a larger electrode, a notch can be machined into the electrode for a thermal measurement device, so the wiring does not affect the chambers.

6.0 References

Advance Cooling Technologies. (n.d.). Spot Cooling Heat Pipes. Retrieved May 18, 2020, from http://www.1-act.com/spot-cooling-heat-pipes/

Belle, O. C., Rip, A., Böttcher, C. J., & Bordewijk, P. (1973). Theory of electric polarization (2nd ed.).

Chu, R. C. (2004). The Challenges of Electronic Cooling: Past, Current and Future. Journal of Electronic Packaging, 126(4), 491-500. doi:10.1115/1.1839594

Demircan, Y., Özgür, E., & Külah, H. (2013). Dielectrophoresis: Applications and future outlook in point of care. Electrophoresis, 34(7), 1008-1027. doi:10.1002/elps.201200446

Dukhin, A., Ulberg, Z., Gruzina, T., & Karamushka, V. (2014). Peculiarities of live cells' interaction with micro- and nanoparticles. Colloid and Interface Science in Pharmaceutical Research and Development, 193-222. doi:10.1016/b978-0-444-62614-1.00010-7

FerroTec. (n.d.). Intro to Thermoelectric Cooling - Thermoelectric. Retrieved May 18, 2020, from https://thermal.ferrotec.com/technology/thermoelectric-reference-guide/thermalref01/

Gascoyne, P. R., Wang, X. B., Huang, Y., & Becker, F. F. (1997). Dielectrophoretic Separation of Cancer Cells from Blood. IEEE transactions on industry applications, 33(3), 670–678. https://doi.org/10.1109/28.585856

GRIMNES, S. (2017). BIOIMPEDANCE AND BIOELECTRICITY BASICS. Place of publication not identified: ELSEVIER ACADEMIC Press.

Jones, L. & Rodgers, A. (2014, January 27). Synthetic jet cooling for small form factor computing. Retrieved May 18, 2020, from http://smallformfactors.mil-embedded.com/articles/synthetic-form-factor-computing/

Jones, L., & Rodgers, A. (2014, January 27). Synthetic jet cooling for small form factor computing. Retrieved May 18, 2020, from http://smallformfactors.mil-embedded.com/articles/synthetic-form-factor-computing/

Lee, S. (1995). Optimum Design and Selection of Heat Sinks. IEEE Transactions on Components, Packaging, and Manufacturing, 18(4).

Leung, S. L., Li, M. L., & Li, W. J. (2008). Formation of gold Nano-particle chains by DEP — a parametric experimental analysis. 3rd IEEE International Conference on Nano/Micro Engineered and Molecular Systems. doi:10.1109/nems.2008.4484496

Lewis, E. (2019, March 02). Methods of Plating Stainless Steel. Retrieved May 18, 2020, from https://sciencing.com/methods-plating-stainless-steel-8741267.html

Mahalingam, R. (2019, July 02). Synthetic jets for forced air cooling of electronics. Retrieved May 18, 2020, from https://www.electronics-cooling.com/2007/05/synthetic-jets-for-forced-air-cooling-of-electronics/

Maxwell, J. (1954). Treatise on Electricity and Magnetism (Reprint ed., Vol. 1). Dover.

Myron L Company. (n.d.). Application Bulletin DEIONIZED WATER [Brochure]. Carlsbad, CA: Author.

Newegg. (n.d.). CPU Cooler. Retrieved May 18, 2020, from http://www.newegg.com/Product/ProductList.asp?Brand=1647

Ozturk, B., Flanders, B. N., Grischkowsky, D. R., & Mishima, T. D. (2007). Single-step growth and low resistance interconnecting of gold nanowires. Nanotechnology, 18(17), 175707. doi:10.1088/0957-4484/18/17/175707

Pamme, Nicole. (2008). Continuous flow separations in microfluidic devices. Lab on a chip. 7. 1644-59. 10.1039/b712784g.

Pethig, R. (2017). Dielectrophoresis: Theory, methodology and biological applications. Hoboken, NJ: John Wiley & Sons.

Repair of burnt smooth motor ... - Data Recovery Ireland. (n.d.). Retrieved May 18, 2020, from https://datarecoveryireland.ie/repair-of-burnt-smooth-motor-controller-chip-on-western-digital-drive/

Rozynek, Z., Han, M., Dutka, F., Garstecki, P., Józefczak, A., & Luijten, E. (2017). Formation of printable granular and colloidal chains through capillary effects and dielectrophoresis. Nature Communications, 8(1). doi:10.1038/ncomms15255

San Jose State Mech Eng Department. (n.d.). Heat Sink Selection. Lecture presented at Thermal Management of Electronics, San Jose.

Sylgard. (n.d.). SYLGARD™ 184 Silicone Elastomer. Retrieved from https://www.dow.com/content/dam/dcc/documents/en-us/productdatasheet/11/11-31/11-3184-sylgard-184-elastomer.pdf?iframe=true

Wagner, R. S., & Ellis, W. C. (1964). Vapor-Liquid-Solid Mechanism Of Single Crystal Growth. Applied Physics Letters, 4(5), 89-90. doi:10.1063/1.1753975

Wang, H., Jewell-Larsen, N. E., & Mamishev, A. V. (2013). Thermal management of microelectronics with electrostatic fluid accelerators. Applied Thermal Engineering, 51(1-2), 190-211. doi:10.1016/j.applthermaleng.2012.08.068

Appendix A: Temperature of Each Electrode Separated by Air

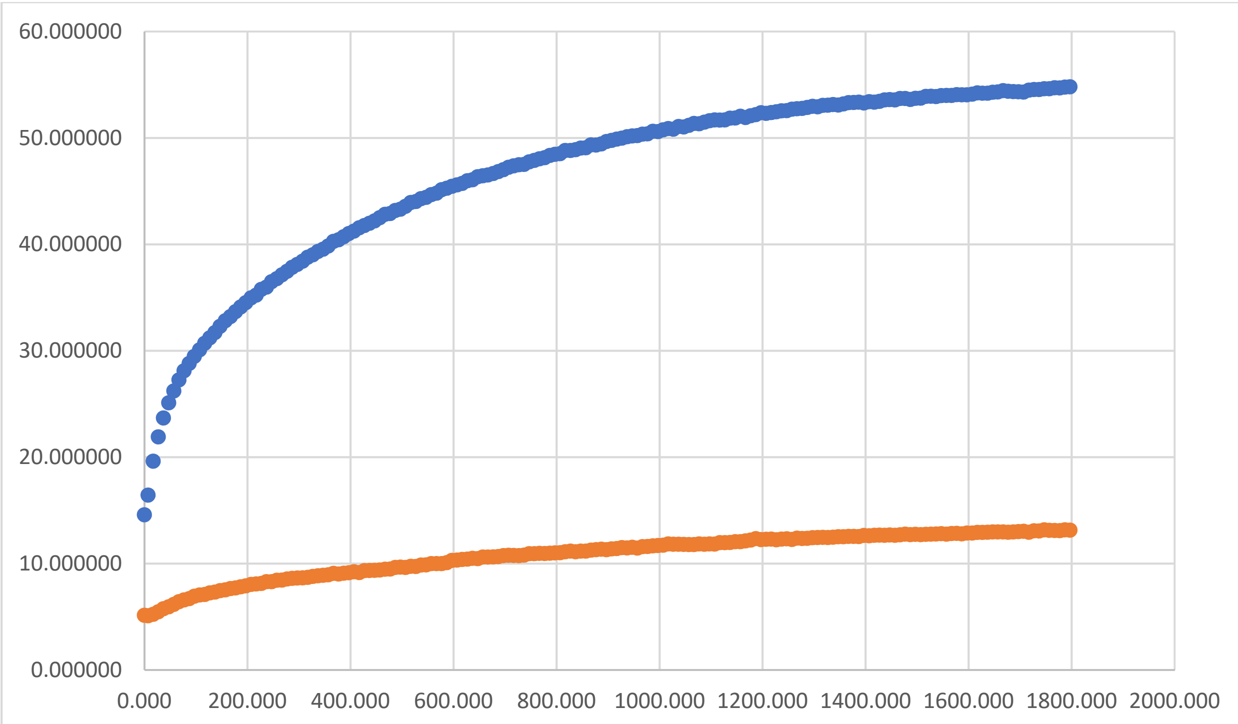

Figure 14 Temperature of electrodes 1 and 2

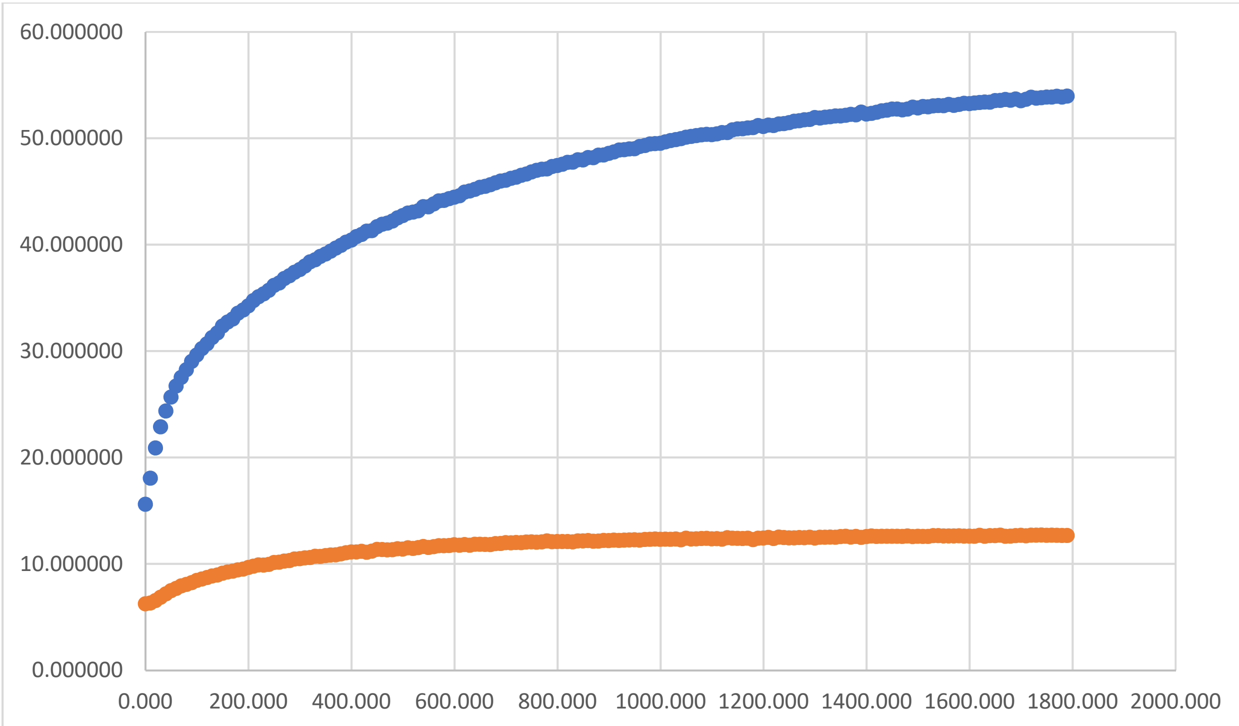

Figure 15 Temperature of electrodes 1 and 2

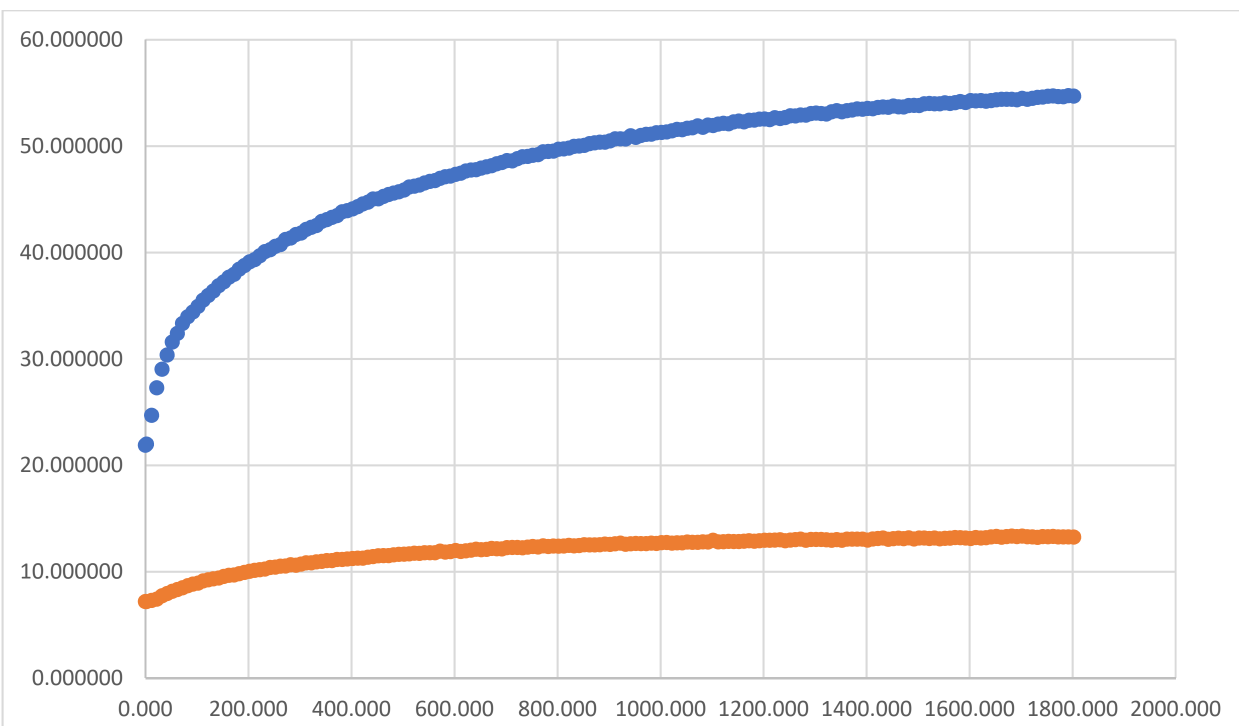

Figure 16 Temperature of electrodes 1 and 2

Appendix B: Temperature of Each Electrode Separated by Water

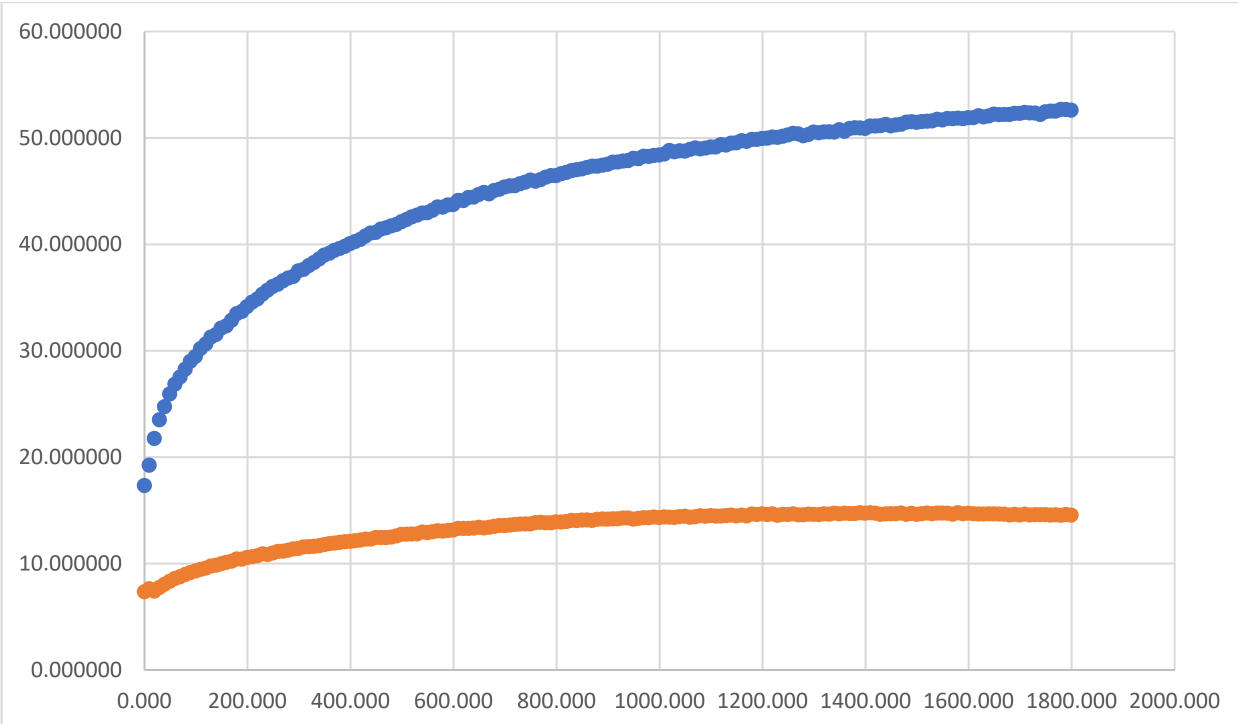

Figure 17 Temperature of electrodes 1 and 2

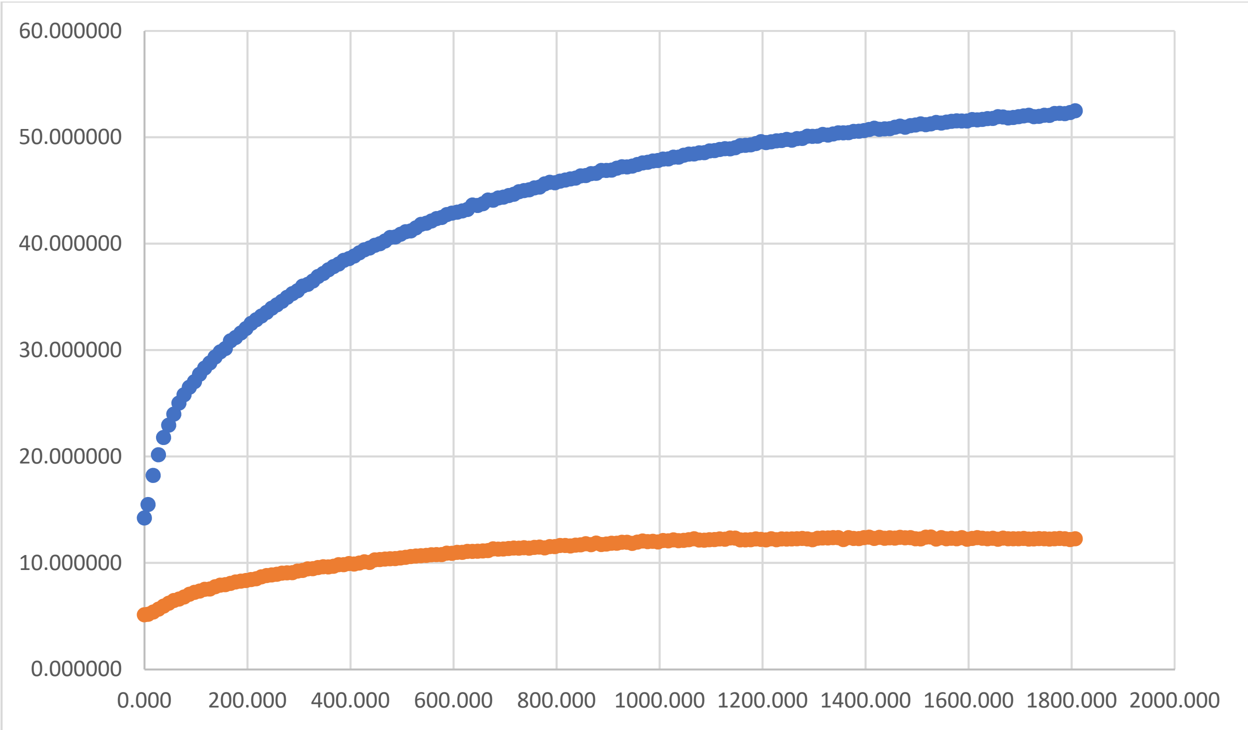

Figure 18 Temperature of electrode 1 and 2

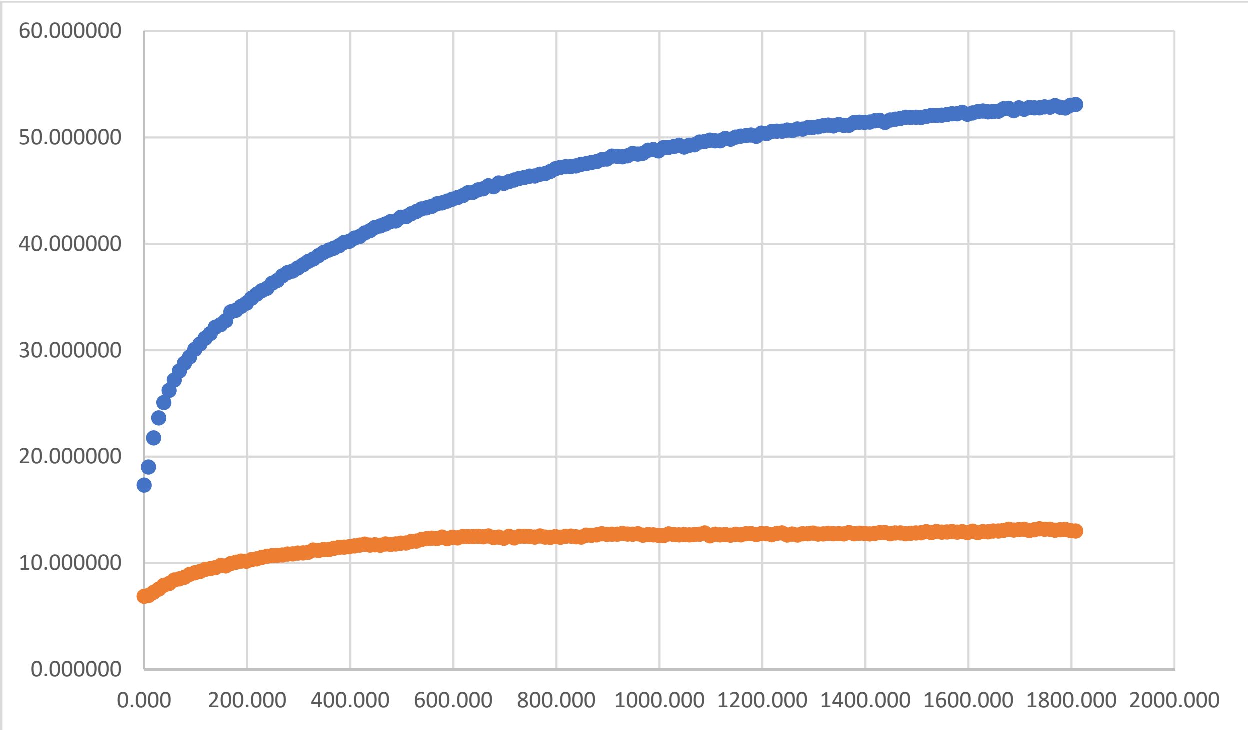

Figure 19 Temperature of electrode 1 and 2

Appendix C: Temperature of Each Electrode Separated by Colloidal Gold

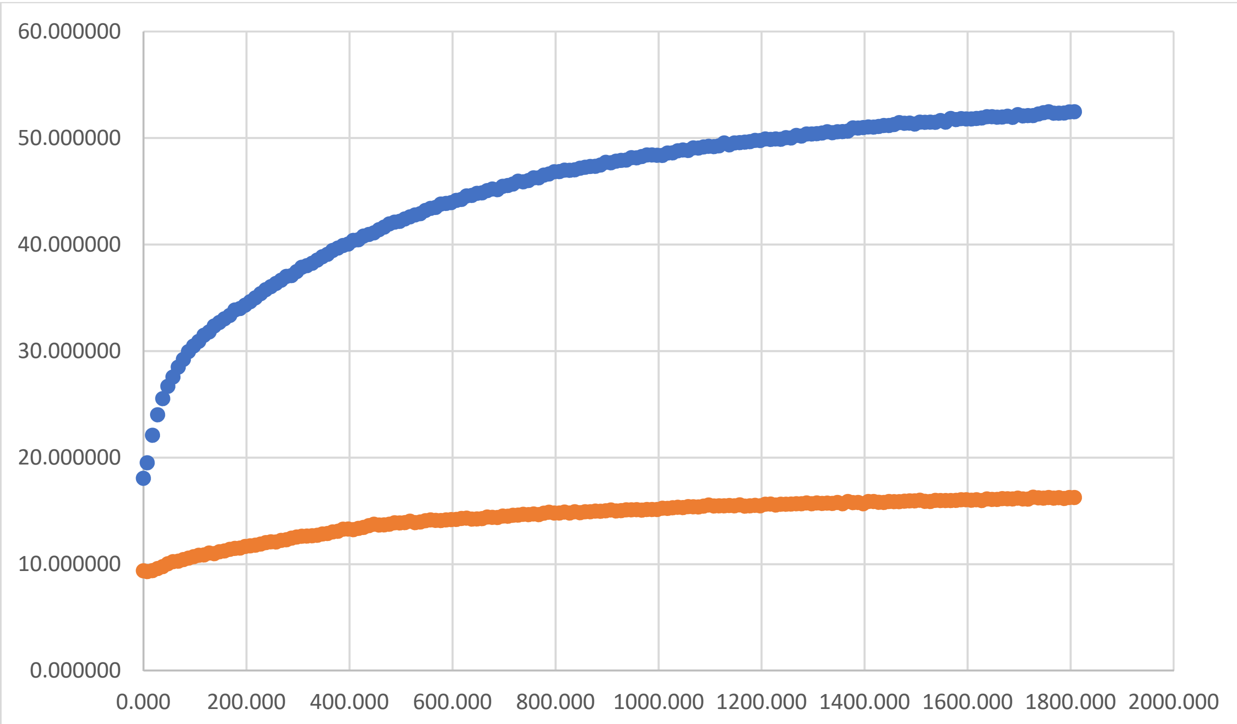

Figure 20 Temperature of electrode 1 and 2

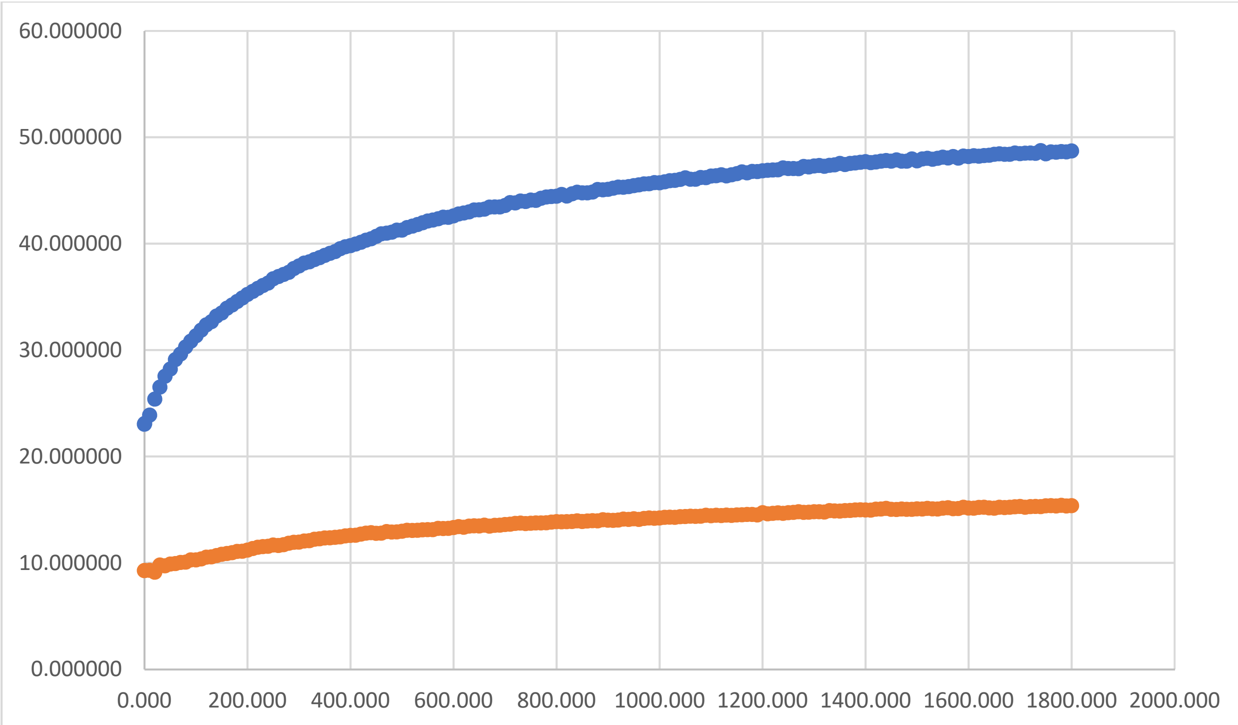

Figure 21 Temperature of electrode 1 and 2

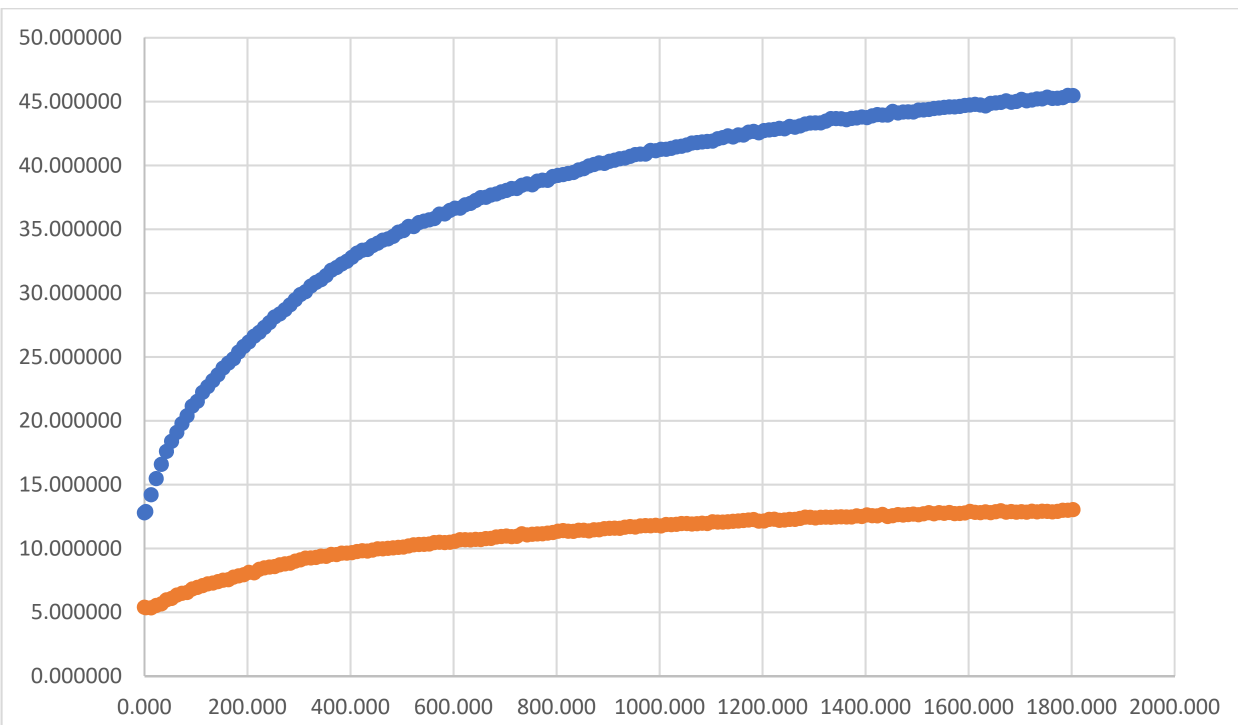

Figure 22 Temperature of electrode 1 and 2

Appendix D: Temperature of Each Electrode Separated by Colloidal Gold with a 3 V, 5 MHz AC Current

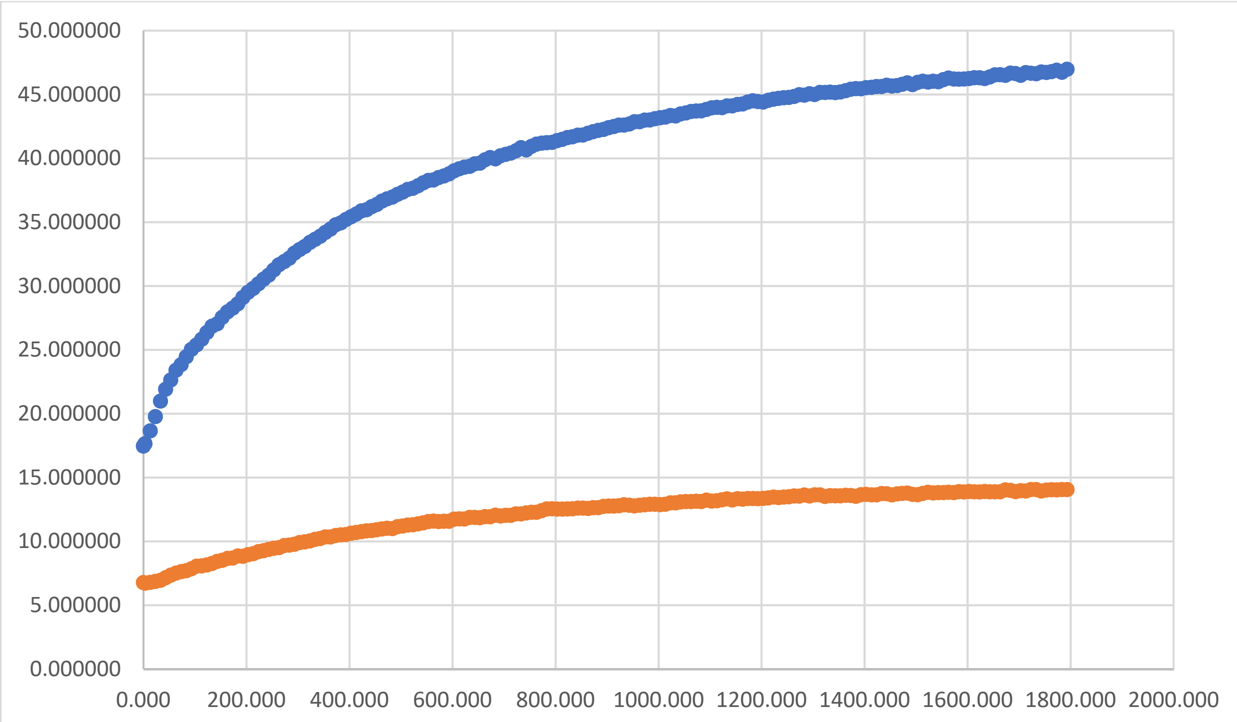

Figure 23 Temperature of electrodes 1 and 2 under a 3V, 5 MHz AC current

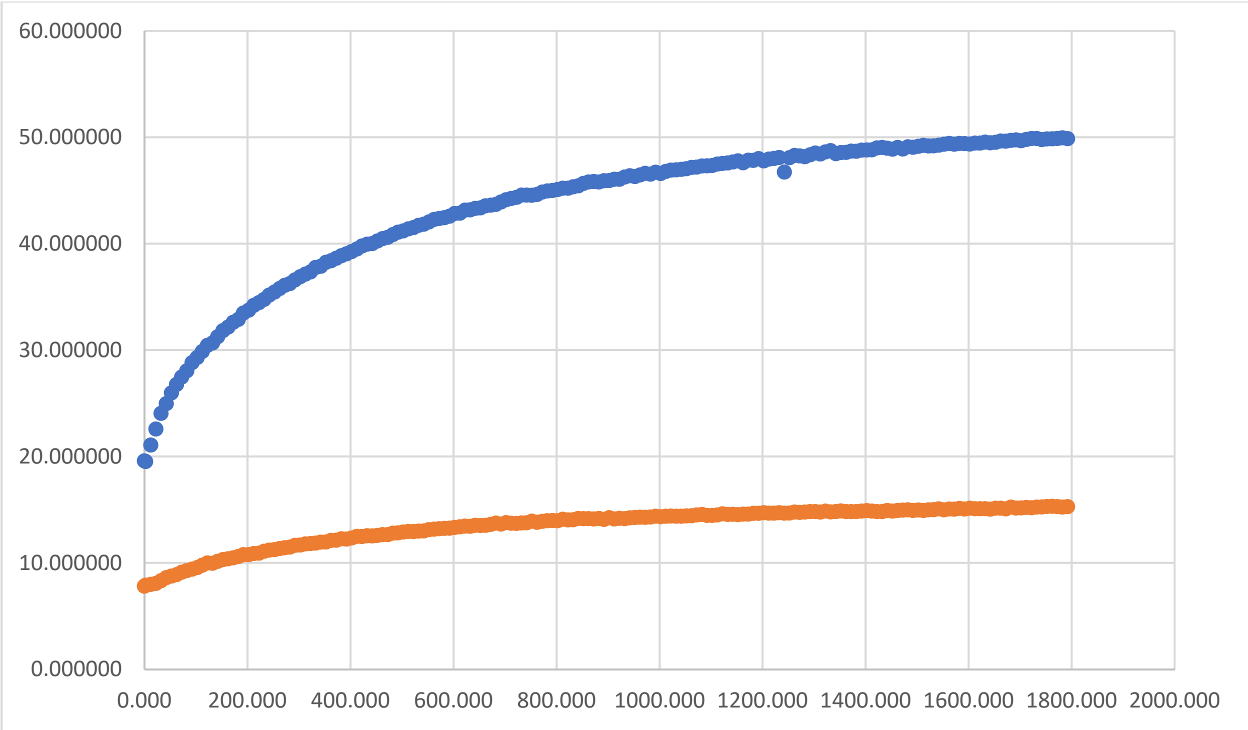

Figure 24 Temperature of electrodes 1 and 2 under a 3V, 5 MHz AC current

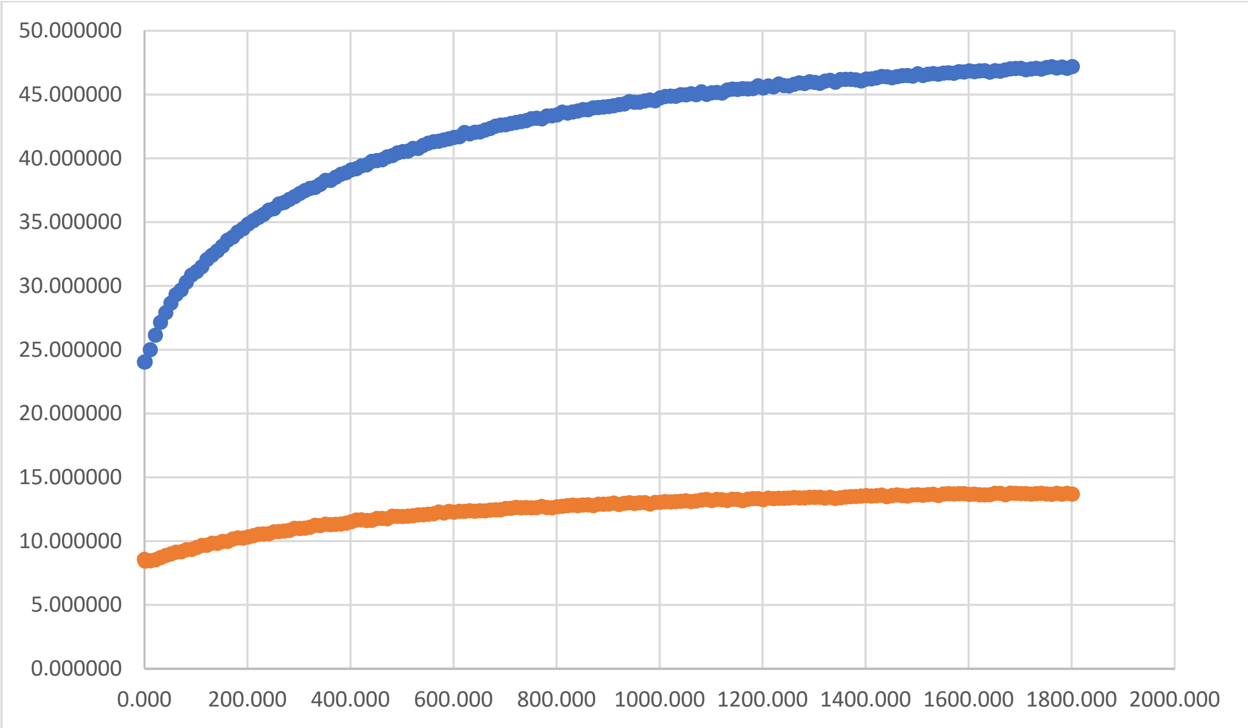

Figure 25 Temperature of electrodes 1 and 2 under a 3V, 5 MHz AC current

Appendix E: Temperature of Each Electrode Separated by Colloidal Gold with a Varying Voltage, 5 MHz AC Current

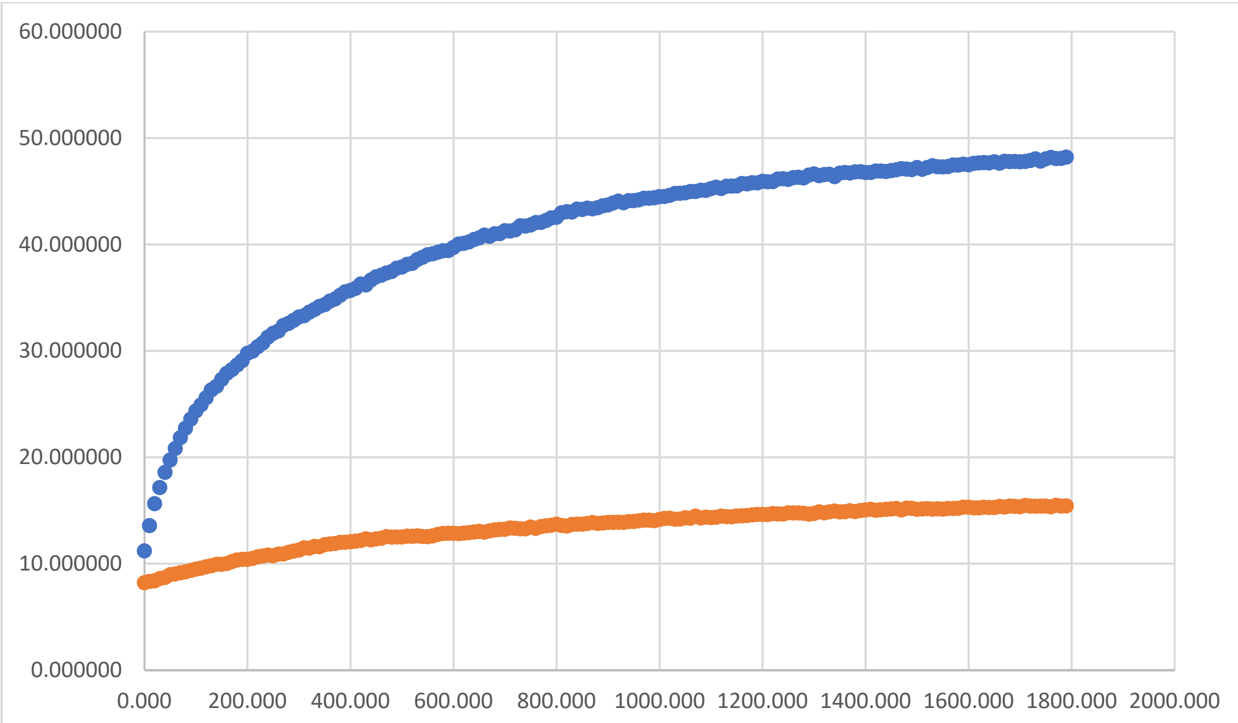

Figure 26 Temperature of electrodes 1 and 2 under a 1.5V, 5 MHz AC current

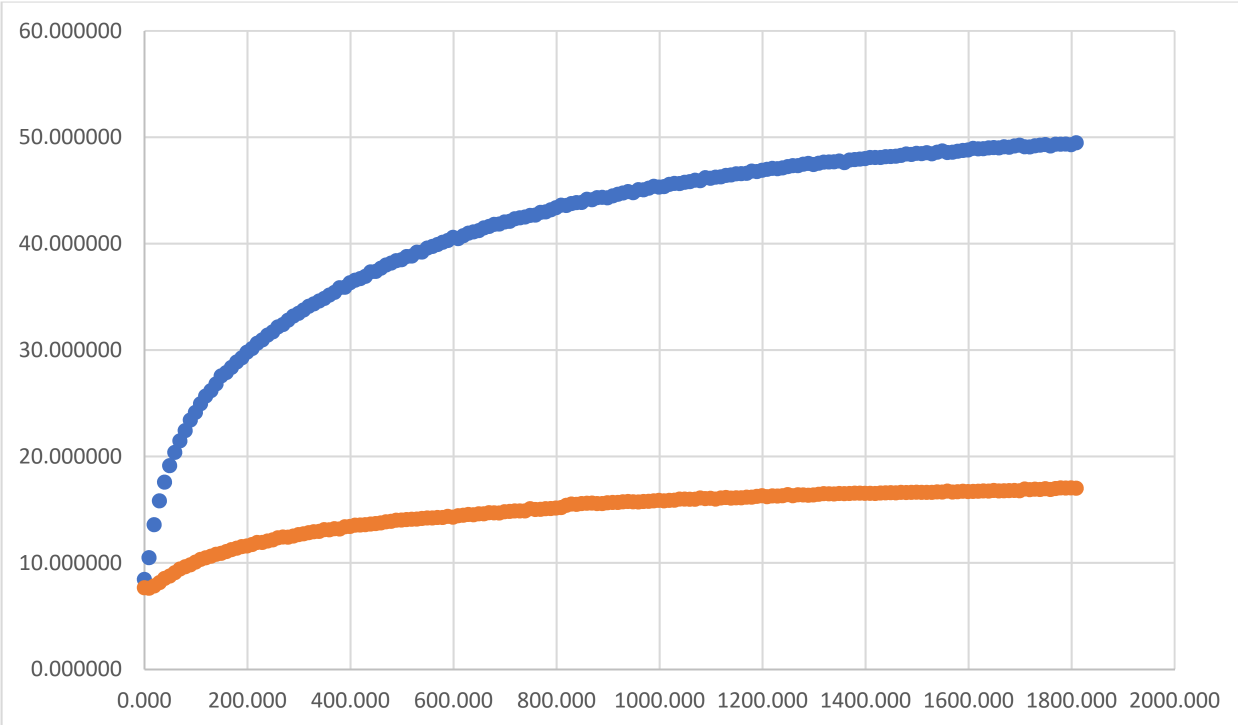

Figure 27 Temperature of electrodes 1 and 2 under a 2V, 5 MHz AC current

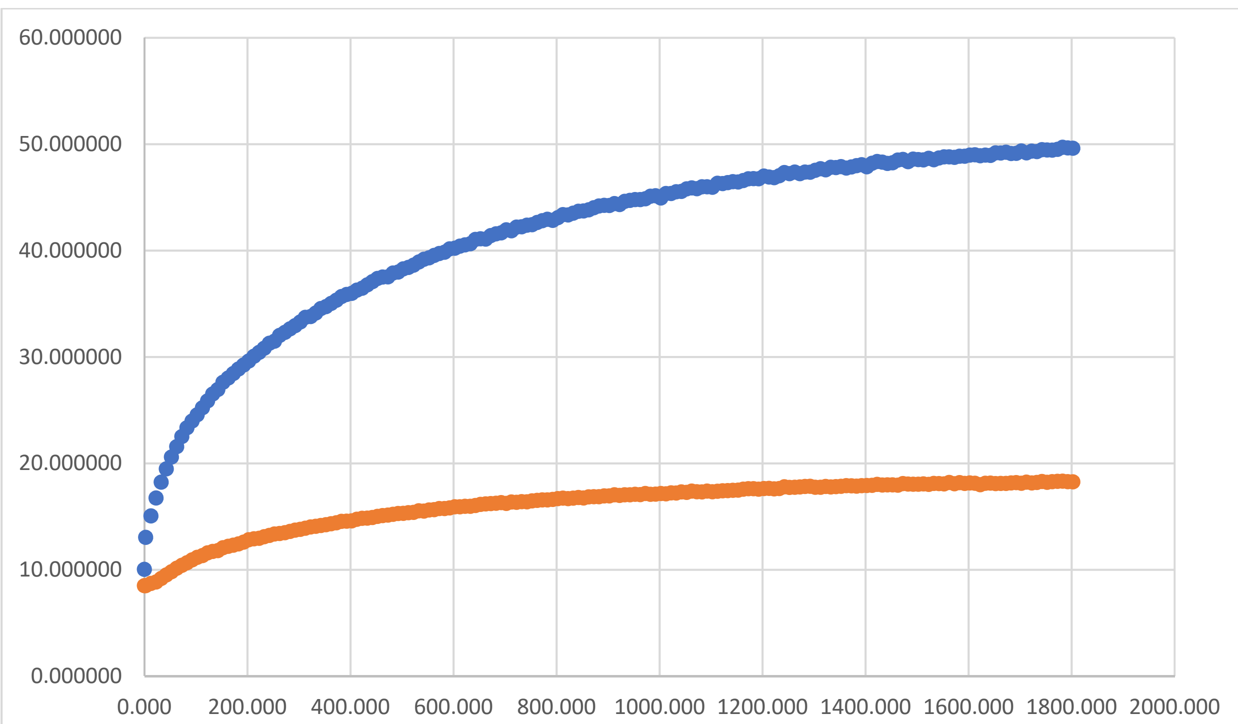

Figure 28 Temperature of electrodes 1 and 2 under a 4V, 5 MHz AC current

Appendix F: Temperature of Each Electrode Separated by Colloidal Gold with a 3 V, Varying Frequency AC Current

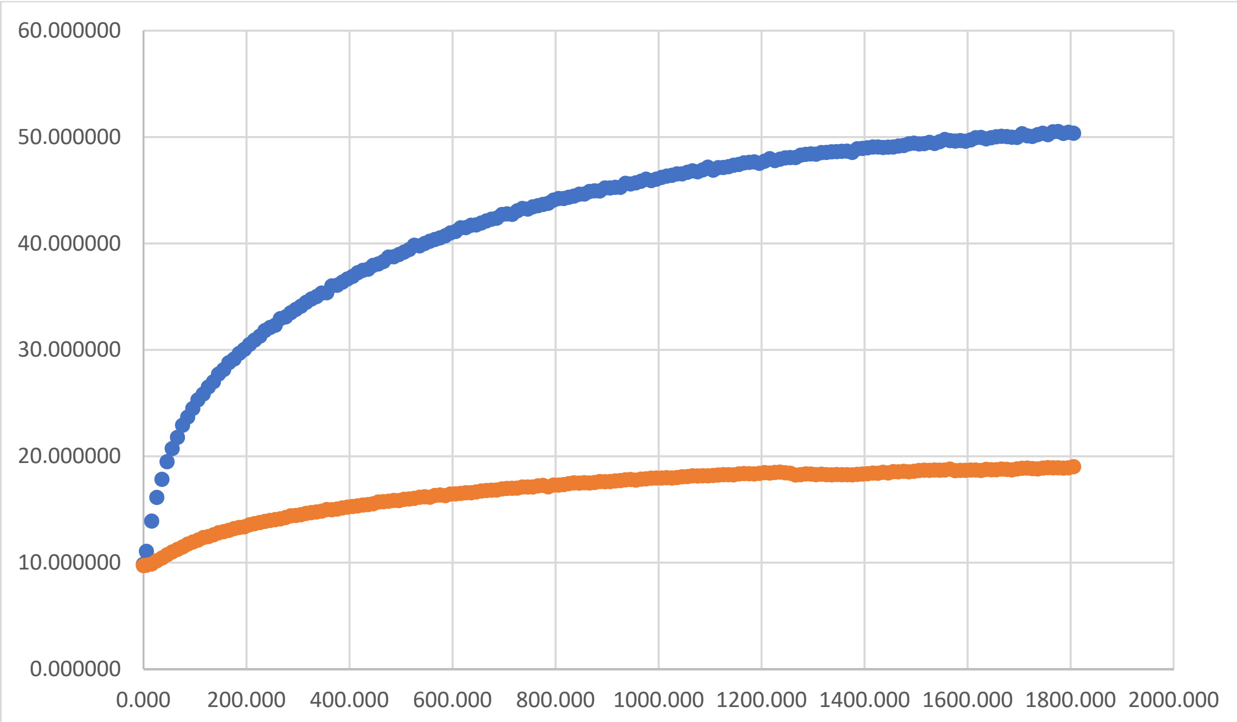

Figure 29 Temperature of electrodes 1 and 2 under a 3V, .1 MHz AC current

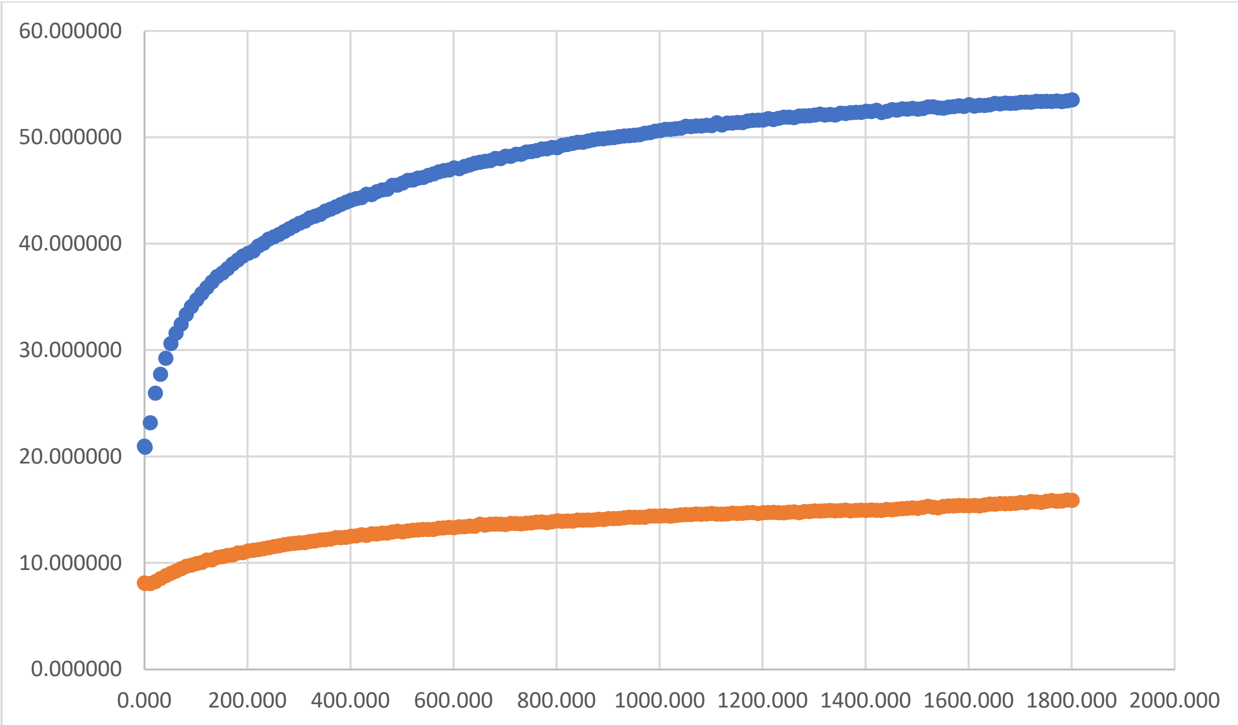

Figure 30 Temperature of electrodes 1 and 2 under a 3V, .5 MHz AC current

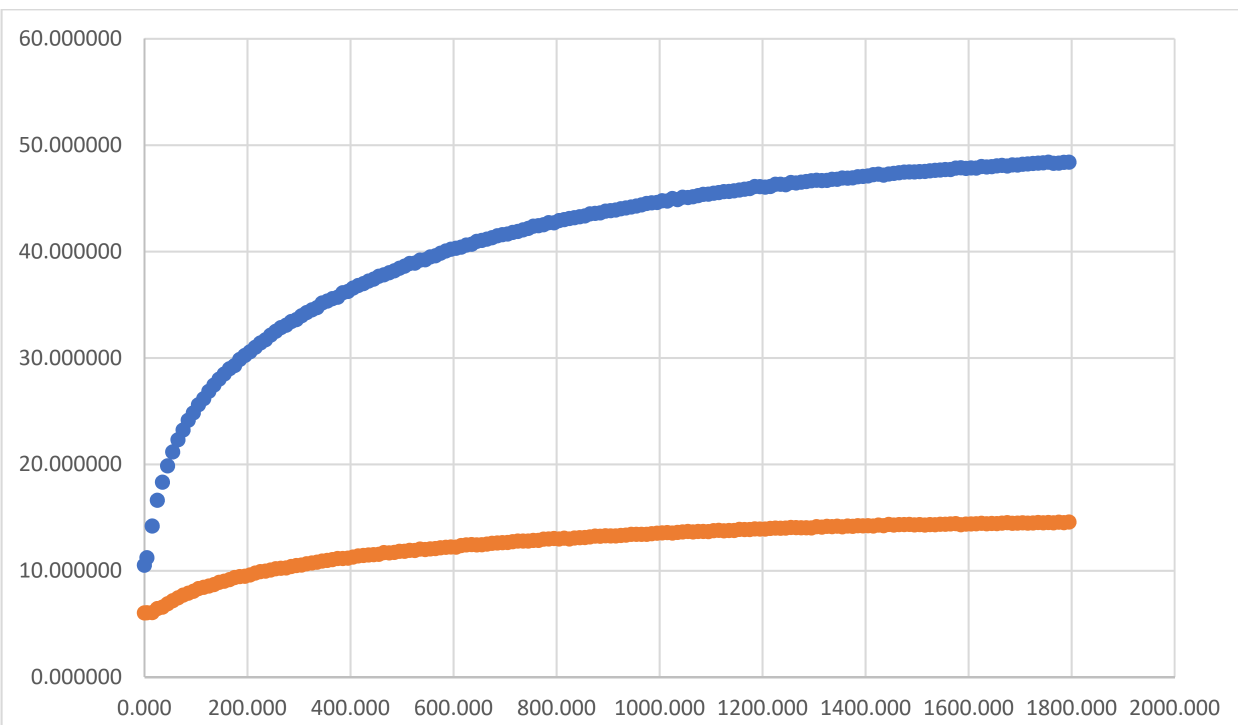

Figure 31 Temperature of electrodes 1 and 2 under a 3V, 1 MHz AC current

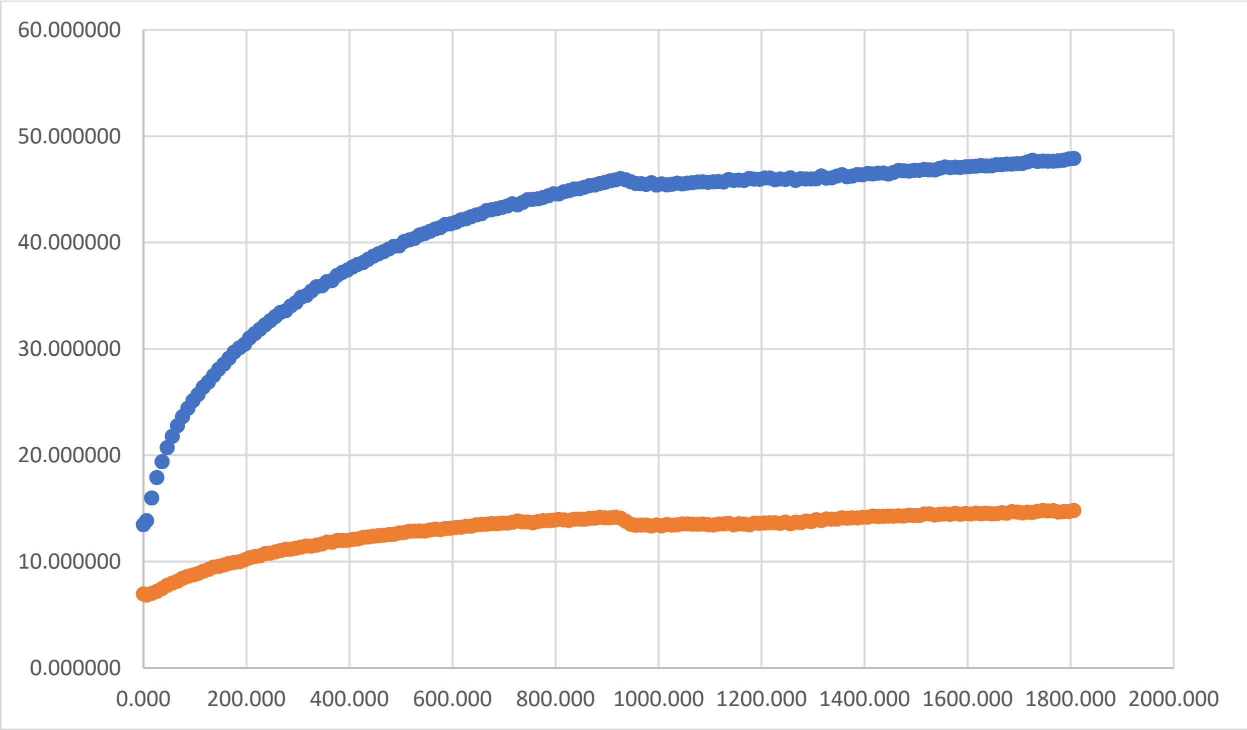

Figure 32 Temperature of electrodes 1 and 2 under a 3V, 3 MHz AC current

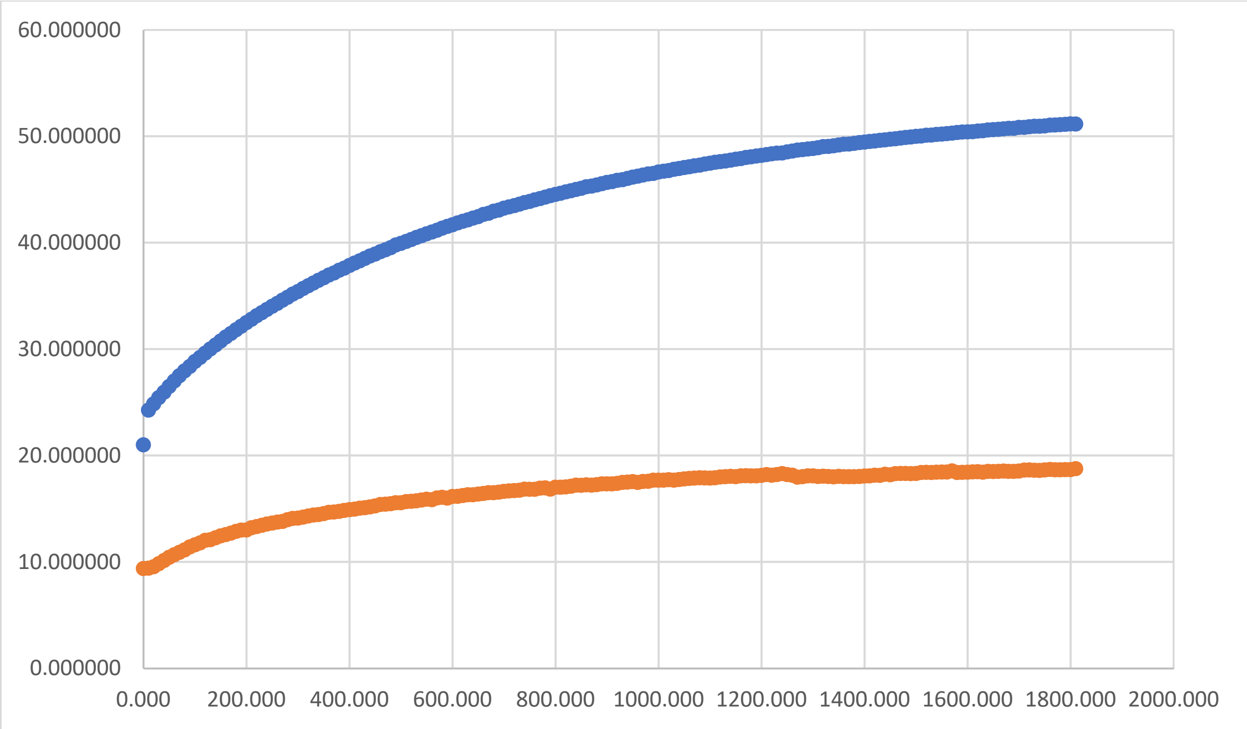

Figure 33 Temperature of electrodes 1 and 2 under a 3V, 6 MHz AC current

Appendix G: Average Temperature Difference of the Two Electrodes

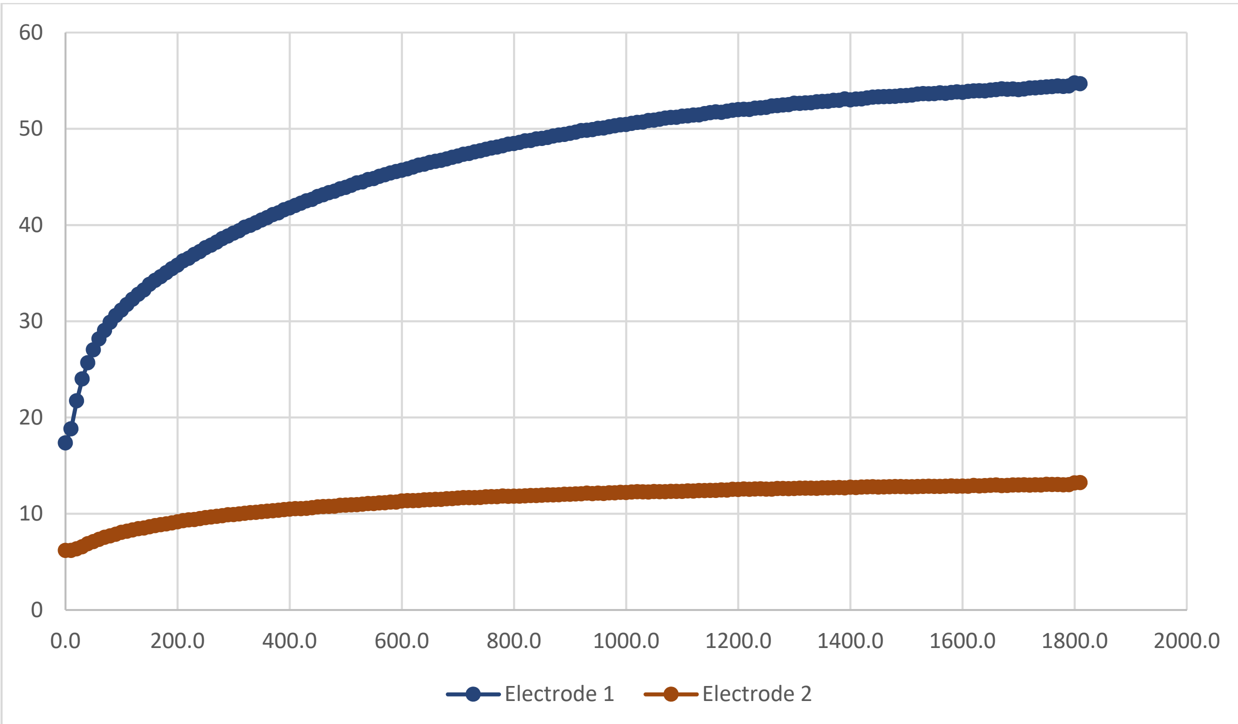

Figure 34 Average temperature of Electrodes 1 and 2 for fluid medium of air

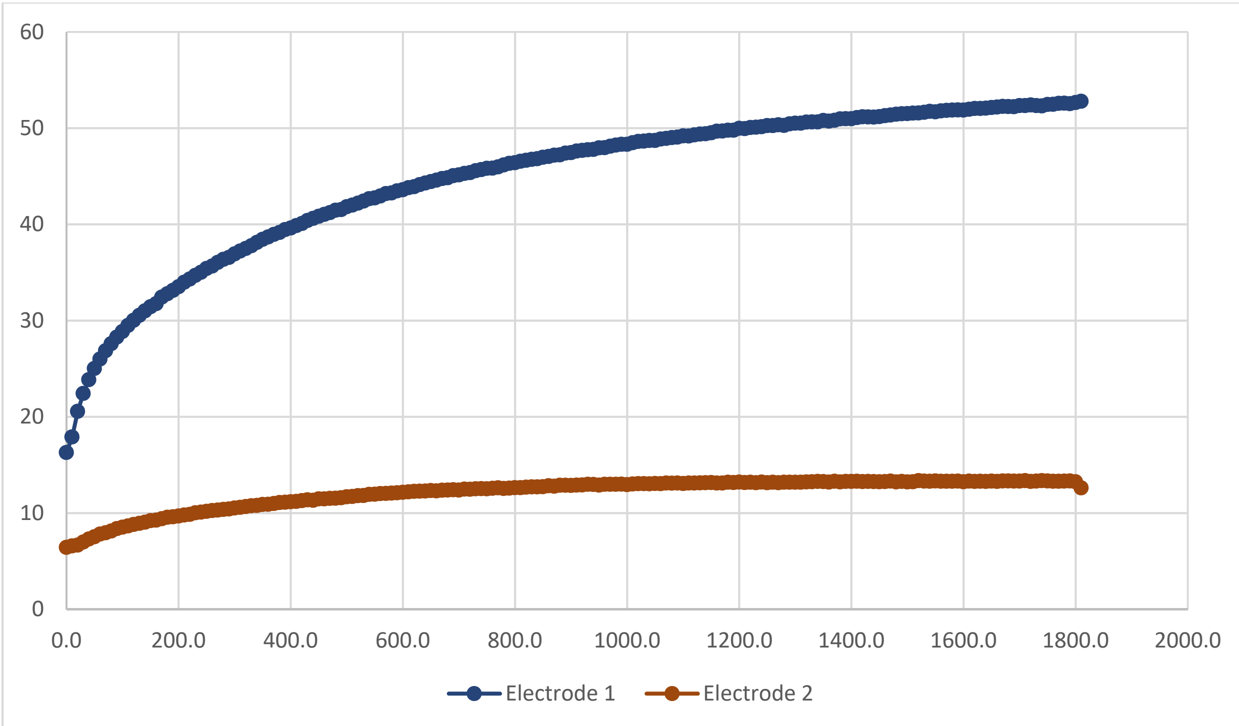

Figure 35 Average temperature of electrodes 1 and 2 for fluid medium of water

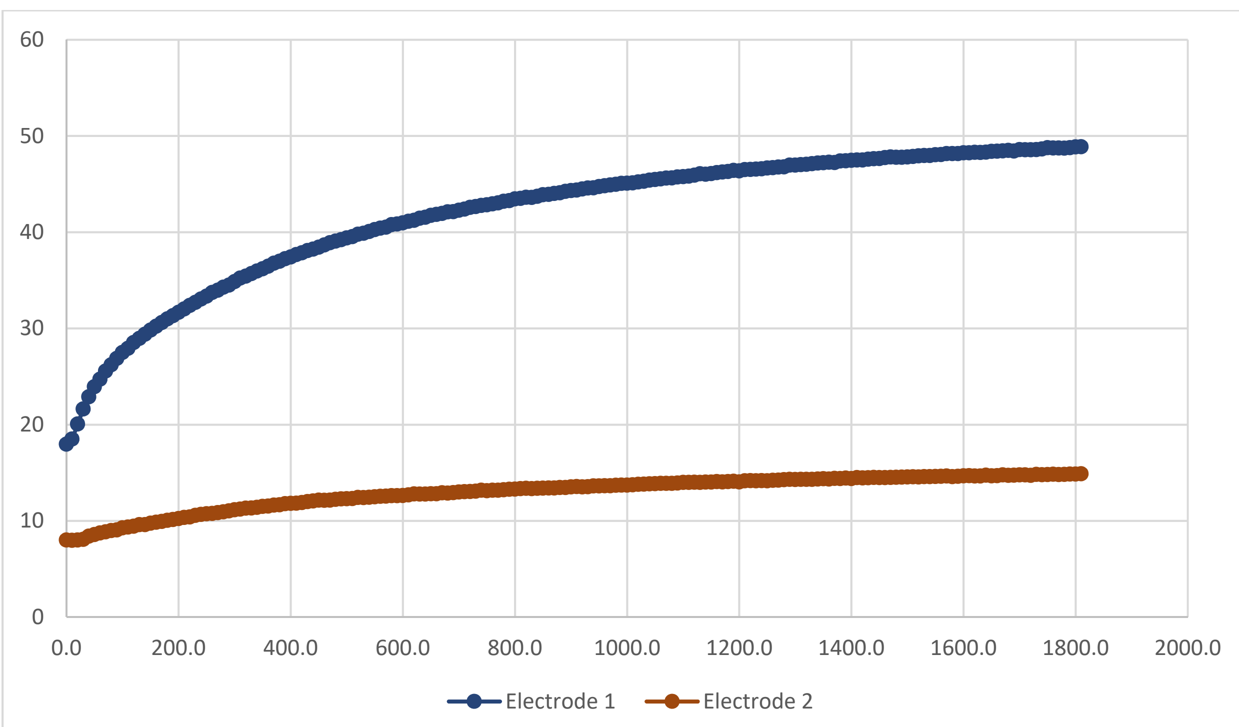

Figure 36 Average temperature of electrodes 1 and 2 for fluid medium of water plus gold

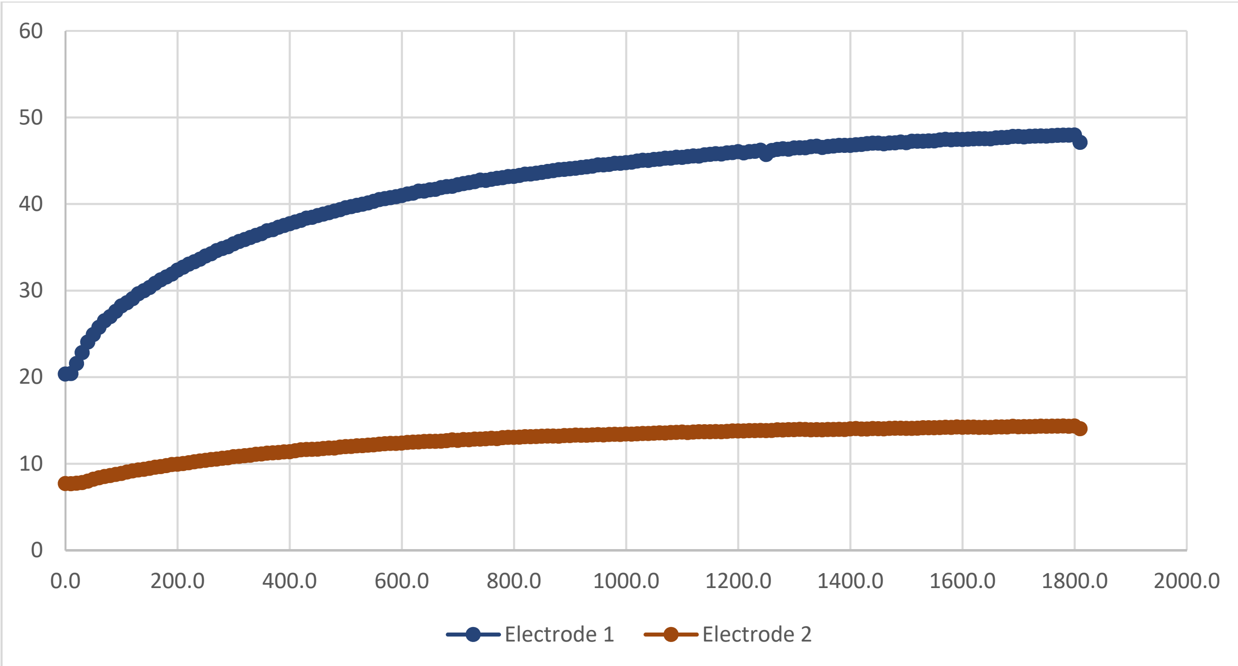

Figure 37 Average temperature of electrodes 1 and 2 for fluid medium of water plus gold under 3V and 5 MHz

Appendix H: Ice Bath Temperature

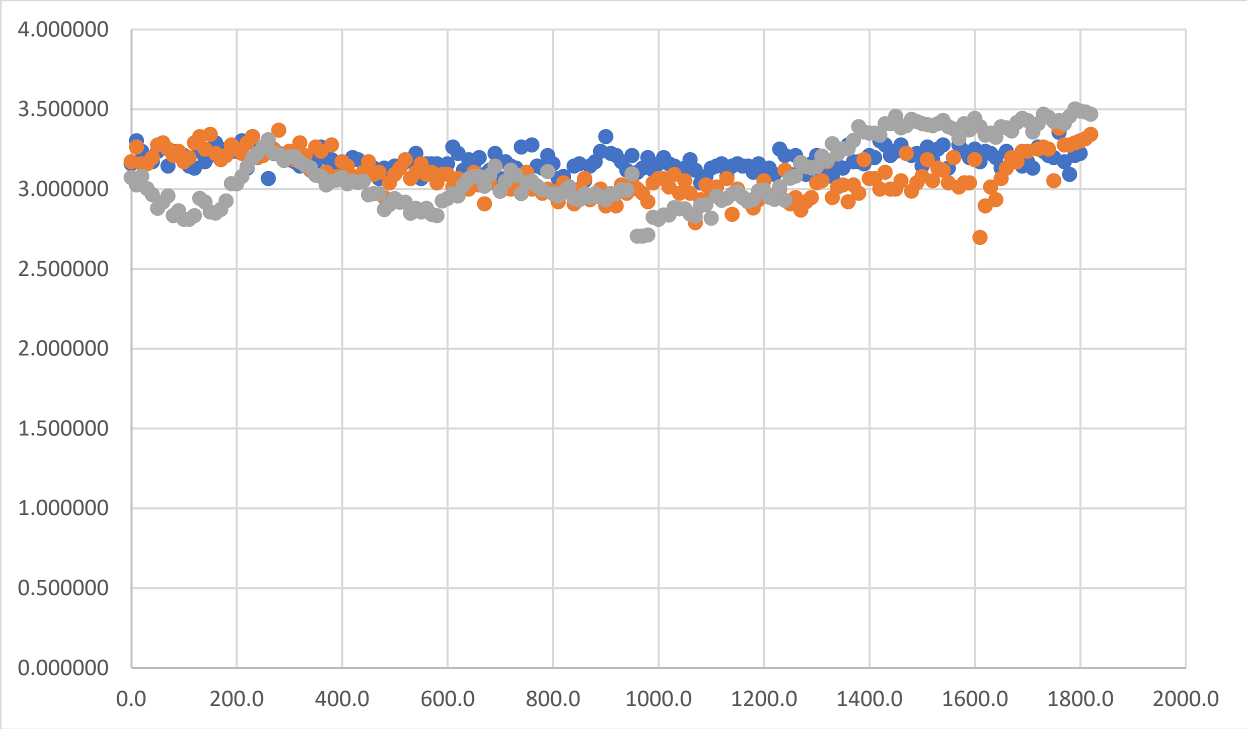

Figure 38 Ice water temperature

Appendix I: Temperature of Electrode 1 for each experiment

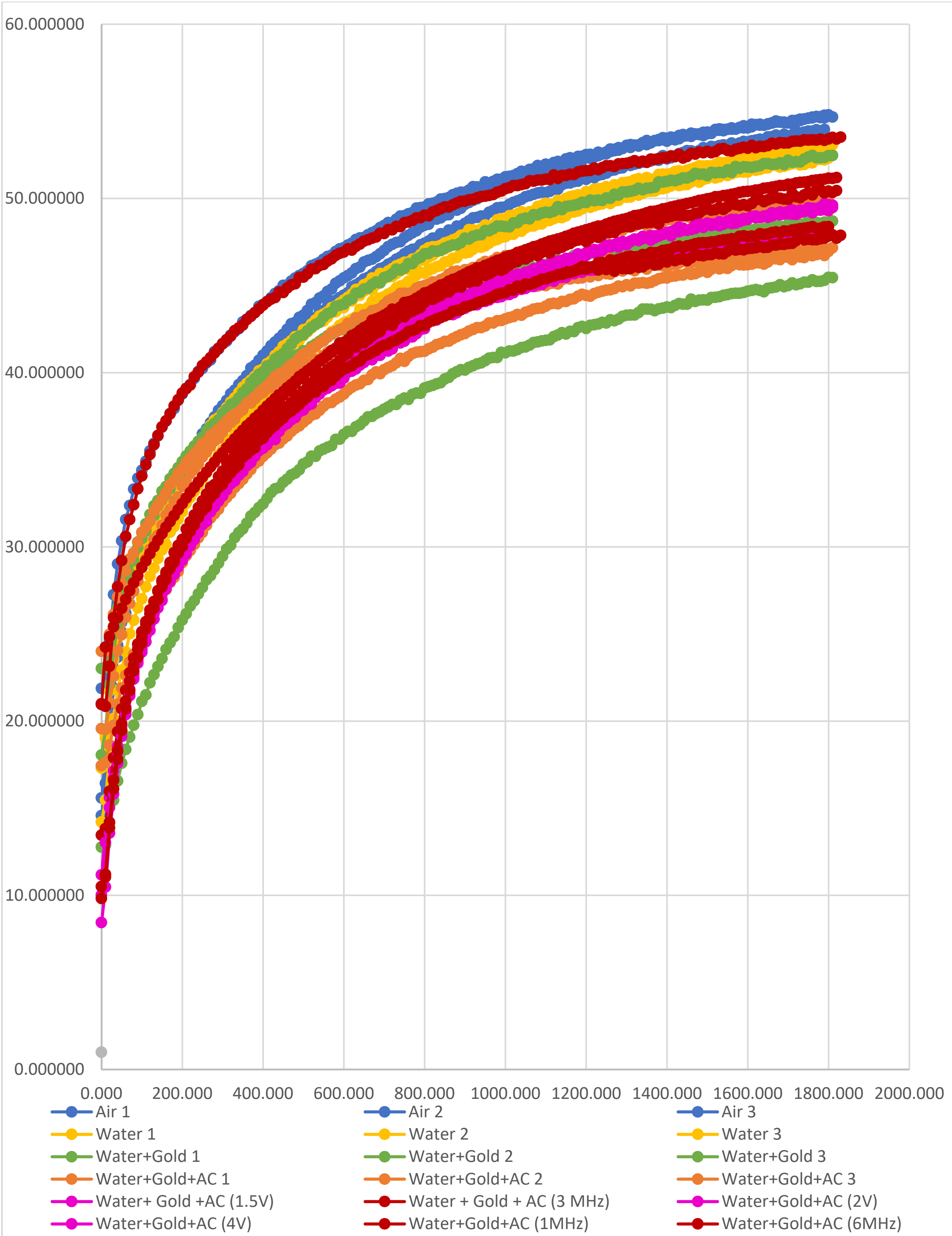

Appendix J: Temperature of Electrode 2 for each experiment

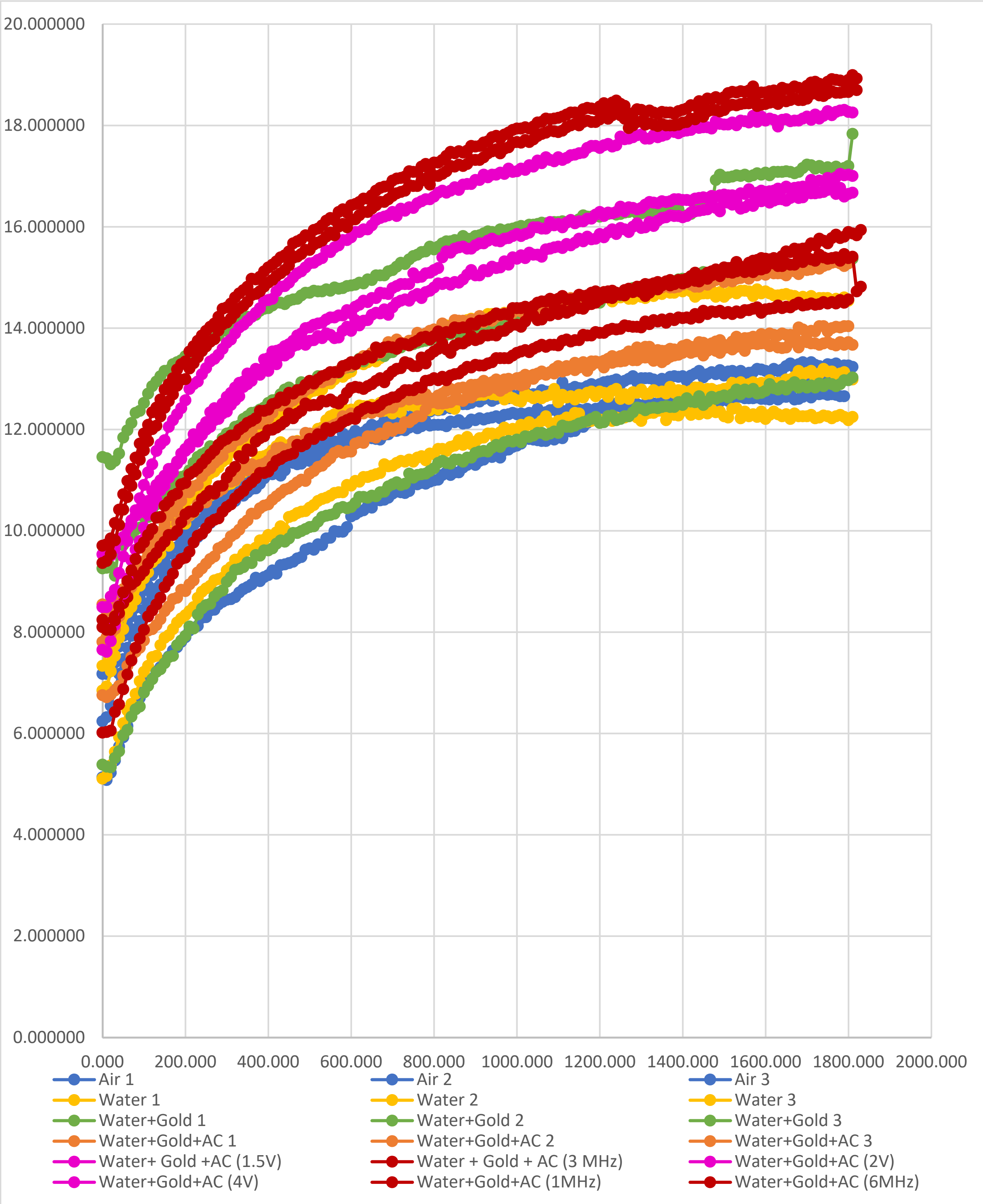

Figure 39 Temperature of Electrode 2

Appendix K: Temperature of the Electrodes at Different Times

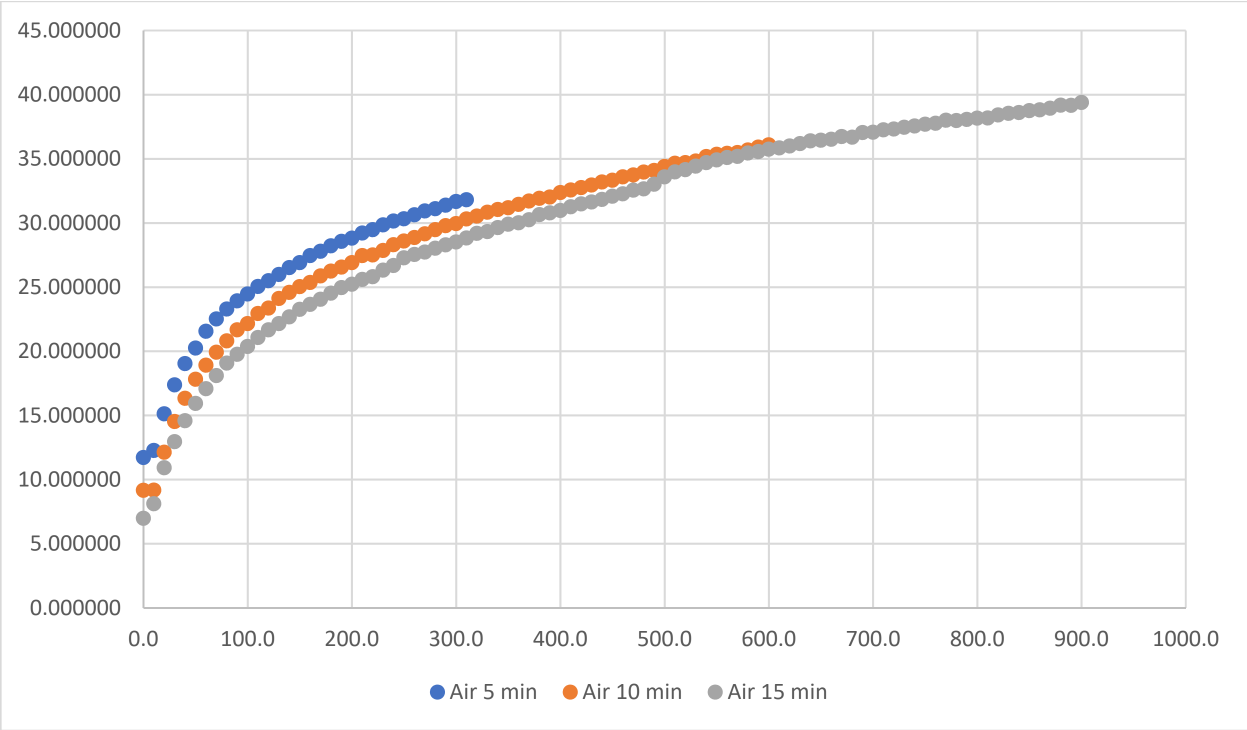

Figure 40 Temperature difference of the electrodes stopped at different times

Appendix L: Bill of Materials

Cooling Chamber:

- Aluminum stock pieces for mold fabrication
- Vacuum chamber
- PDMS Sylgard 184 Silicon Elastomer 2-part mix
- 2 acrylic plates
- 10 bolts, 10 nuts, and 20 washers

Electrodes: **web links?>**

- Stainless Steel 316SS
- Caswell Stainless Steel Activator for gold
- Caswell 24K gold solution
- Midas Acid Dip and Electrocleaning solution
- 2 Omega SA1-Platinum RTDs

Ice Bath:

- Ice
- 1.8 mm ID PTFE Tubing
- 12 VDC micro pump
- 9VDC power supply

Fluid Mediums:

- Deionized water
- Gold 300-500 μm microparticles
- Dual Channel DDS Signal Generator/Counter

Heating Element:

- Copper Plate
- Thermal Paste: 5 W/mK
- Polyimide Insulated Flexible Heater: KHLVA-0502/10-P

- BK Precision 1550 DC Power Supply

Data Acquisition:

- LabJack U6-Pro
- Spare wiring for circuit
- LJLogUD LabView Program

Appendix M: Data Table Example

Example data table showing the recorded values of time, voltages before/after each RTD, and the calculated values of the temperature at each RTD.

Air Test 1									
Time	**Time**	**Before RTD1**	**After RTD1**	**Resistance 1**	**Temp 1**	**Before RTD2**	**After RTD2**	**Resistance 2**	**Temp 2**
3670537686.759	0.000	0.040938	0.020114	105.612837	14.578799	0.020115	0.000008	101.976437	5.133602
3670537693.887	7.128	0.041073	0.020109	106.322874	16.423049	0.020108	0.000005	101.956150	5.080910
3670537703.887	17.128	0.041323	0.020117	107.550222	19.610967	0.020120	0.000006	102.011939	5.225815
3670537713.888	27.129	0.041520	0.020140	108.432696	21.903107	0.020138	0.000006	102.103229	5.462933
3670537723.887	37.128	0.041676	0.020162	109.112302	23.668318	0.020158	0.000005	102.209735	5.739570
3670537733.889	47.130	0.041805	0.020182	109.665116	25.104198	0.020172	0.000005	102.280738	5.923995
3670537743.887	57.128	0.041903	0.020196	110.091138	26.210749	0.020190	0.000006	102.366957	6.147940
3670537753.888	67.129	0.041994	0.020208	110.491802	27.251433	0.020210	0.000006	102.468391	6.411404
3670537763.886	77.127	0.042071	0.020220	110.821461	28.107692	0.020222	0.000006	102.529251	6.569483
3670537773.887	87.128	0.042134	0.020230	111.090261	28.805872	0.020231	0.000005	102.579968	6.701215
3670537783.887	97.128	0.042196	0.020242	111.343845	29.464533	0.020247	0.000005	102.661115	6.911987
3670537793.886	107.127	0.042254	0.020254	111.577143	30.070501	0.020257	0.000005	102.711832	7.043719
3670537803.887	117.128	0.042309	0.020262	111.815512	30.689642	0.020261	0.000006	102.727047	7.083238
3670537813.887	127.128	0.042364	0.020278	112.013308	31.203398	0.020272	0.000006	102.782835	7.228144

3670537823.888	137.129	0.042406	0.020282	112.206032	31.703980	0.020278	0.000006	102.813266	7.307183
3670537833.890	147.131	0.042458	0.020290	112.429187	32.283601	0.020288	0.000006	102.863982	7.438915
3670537843.887	157.128	0.042503	0.020295	112.632054	32.810530	0.020292	0.000004	102.894413	7.517955
3670537853.885	167.126	0.042543	0.020305	112.784205	33.205727	0.020302	0.000005	102.940058	7.636514
3670537863.888	177.129	0.042587	0.020314	112.961714	33.666789	0.020307	0.000005	102.965416	7.702380
3670537873.888	187.129	0.042624	0.020318	113.129080	34.101505	0.020315	0.000005	103.005990	7.807765
3670537883.888	197.129	0.042667	0.020330	113.286302	34.509875	0.020322	0.000005	103.041491	7.899978
3670537893.887	207.128	0.042701	0.020329	113.463811	34.970938	0.020333	0.000006	103.092208	8.031710
3670537903.887	217.128	0.042732	0.020341	113.560173	35.221229	0.020337	0.000006	103.112495	8.084403
3670537913.888	227.129	0.042772	0.020340	113.768112	35.761331	0.020339	0.000005	103.127710	8.123923
3670537923.888	237.129	0.042801	0.020353	113.849259	35.972102	0.020352	0.000006	103.188570	8.282001
3670537933.889	247.130	0.042843	0.020356	114.047055	36.485857	0.020354	0.000007	103.193642	8.295174
3670537943.887	257.128	0.042869	0.020360	114.158632	36.775668	0.020363	0.000006	103.244359	8.426907
3670537953.887	267.128	0.042903	0.020367	114.295568	37.131345	0.020364	0.000006	103.249431	8.440080
3670537963.889	277.130	0.042932	0.020371	114.422360	37.460675	0.020372	0.000006	103.290004	8.545465
3670537973.890	287.131	0.042960	0.020370	114.569439	37.842699	0.020375	0.000005	103.310291	8.598158
3670537983.888	297.129	0.042985	0.020375	114.670873	38.106163	0.020379	0.000006	103.325506	8.637678

3670537993.886	307.127	0.043016	0.020383	114.787522	38.409147	0.020380	0.000006	103.330578	8.650851
3670538003.888	317.129	0.043048	0.020386	114.934601	38.791170	0.020383	0.000006	103.345793	8.690371
3670538013.889	327.130	0.043069	0.020391	115.015748	39.001942	0.020389	0.000005	103.381295	8.782583
3670538023.886	337.127	0.043094	0.020392	115.137468	39.318099	0.020395	0.000006	103.406653	8.848449
3670538033.888	347.129	0.043118	0.020399	115.223687	39.542044	0.020397	0.000005	103.421868	8.887969
3670538043.889	357.130	0.043144	0.020403	115.335264	39.831854	0.020401	0.000005	103.442155	8.940662
3670538053.890	367.131	0.043175	0.020401	115.502630	40.266571	0.020412	0.000006	103.492872	9.072394
3670538063.889	377.130	0.043197	0.020411	115.563490	40.424649	0.020407	0.000006	103.467513	9.006528
3670538073.886	387.127	0.043220	0.020412	115.675067	40.714460	0.020413	0.000006	103.497943	9.085567
3670538083.889	397.130	0.043248	0.020418	115.786644	41.004271	0.020417	0.000007	103.513158	9.125087
3670538093.887	407.128	0.043270	0.020422	115.877935	41.241389	0.020423	0.000006	103.548660	9.217300
3670538103.888	417.129	0.043298	0.020427	115.994583	41.544373	0.020419	0.000007	103.523302	9.151433
3670538113.884	427.125	0.043316	0.020429	116.075730	41.755144	0.020430	0.000005	103.589234	9.322685
3670538123.886	437.127	0.043338	0.020434	116.161949	41.979089	0.020434	0.000008	103.594306	9.335858
3670538133.886	447.127	0.043360	0.020439	116.248168	42.203033	0.020435	0.000007	103.604449	9.362205
3670538143.885	457.126	0.043381	0.020438	116.359745	42.492844	0.020436	0.000006	103.614592	9.388551
3670538153.886	467.127	0.043407	0.020440	116.481466	42.809001	0.020442	0.000007	103.639951	9.454417

3670538163.889	477.130	0.043423	0.020450	116.511896	42.888041	0.020444	0.000007	103.650094	9.480764
3670538173.887	487.128	0.043446	0.020451	116.623473	43.177851	0.020454	0.000006	103.705883	9.625669
3670538183.887	497.128	0.043460	0.020456	116.669118	43.296410	0.020457	0.000007	103.716026	9.652016
3670538193.886	507.127	0.043485	0.020460	116.775623	43.573048	0.020456	0.000008	103.705883	9.625669
3670538203.887	517.128	0.043509	0.020457	116.912559	43.928725	0.020462	0.000006	103.746456	9.731055
3670538213.886	527.127	0.043525	0.020466	116.948061	44.020937	0.020462	0.000007	103.741384	9.717882
3670538223.888	537.129	0.043548	0.020469	117.049495	44.284402	0.020472	0.000007	103.792101	9.849614
3670538233.886	547.127	0.043561	0.020473	117.095140	44.402961	0.020472	0.000006	103.797173	9.862787
3670538243.889	557.130	0.043587	0.020479	117.196574	44.666425	0.020482	0.000006	103.847890	9.994519
3670538253.890	567.131	0.043601	0.020483	117.247290	44.798157	0.020482	0.000007	103.842818	9.981346
3670538263.887	577.128	0.043624	0.020481	117.374083	45.127487	0.020480	0.000005	103.842818	9.981346
3670538273.887	587.128	0.043642	0.020488	117.429871	45.272393	0.020488	0.000006	103.878320	10.073559
3670538283.886	597.127	0.043668	0.020501	117.495803	45.443645	0.020504	0.000006	103.959467	10.284330
3670538293.887	607.128	0.043688	0.020511	117.546520	45.575377	0.020509	0.000008	103.974682	10.323850
3670538303.888	617.129	0.043699	0.020511	117.602309	45.720282	0.020512	0.000007	103.994969	10.376543
3670538313.888	627.129	0.043721	0.020514	117.698671	45.970573	0.020514	0.000007	104.005112	10.402889
3670538323.887	637.128	0.043735	0.020521	117.734173	46.062786	0.020519	0.000006	104.035542	10.481928

3670538333.886	647.127	0.043755	0.020519	117.845750	46.352597	0.020518	0.000007	104.025399	10.455582
3670538343.887	657.128	0.043767	0.020524	117.881251	46.444809	0.020528	0.000006	104.081188	10.600487
3670538353.889	667.130	0.043782	0.020534	117.906610	46.510675	0.020528	0.000006	104.081188	10.600487
3670538363.885	677.126	0.043795	0.020536	117.962399	46.655581	0.020530	0.000007	104.086259	10.613660
3670538373.887	687.128	0.043813	0.020541	118.028330	46.826832	0.020532	0.000006	104.101474	10.653180
3670538383.887	697.128	0.043825	0.020539	118.099334	47.011257	0.020538	0.000006	104.131904	10.732219
3670538393.887	707.128	0.043839	0.020536	118.185553	47.235202	0.020541	0.000006	104.147120	10.771739
3670538403.886	717.127	0.043852	0.020539	118.236270	47.366934	0.020541	0.000007	104.142048	10.758566
3670538413.888	727.129	0.043860	0.020539	118.276843	47.472320	0.020540	0.000007	104.136976	10.745393
3670538423.889	737.130	0.043872	0.020548	118.292058	47.511840	0.020543	0.000007	104.152191	10.784912
3670538433.888	747.129	0.043892	0.020550	118.383349	47.748957	0.020553	0.000007	104.202908	10.916644
3670538443.886	757.127	0.043902	0.020550	118.434066	47.880690	0.020551	0.000005	104.202908	10.916644
3670538453.888	767.129	0.043918	0.020555	118.489854	48.025595	0.020554	0.000006	104.213051	10.942991
3670538463.887	777.128	0.043933	0.020561	118.535499	48.144154	0.020554	0.000007	104.207980	10.929818
3670538473.886	787.127	0.043946	0.020558	118.616646	48.354925	0.020557	0.000007	104.223195	10.969337
3670538483.887	797.128	0.043953	0.020557	118.657220	48.460311	0.020558	0.000006	104.233338	10.995684
3670538493.886	807.127	0.043961	0.020561	118.677507	48.513004	0.020560	0.000007	104.238410	11.008857

3670538503.887	817.128	0.043987	0.020564	118.794155	48.815988	0.020566	0.000006	104.273912	11.101069
3670538513.888	827.129	0.043991	0.020568	118.794155	48.815988	0.020571	0.000007	104.294198	11.153762
3670538523.886	837.127	0.044000	0.020572	118.819514	48.881854	0.020566	0.000006	104.273912	11.101069
3670538533.886	847.127	0.044012	0.020572	118.880374	49.039933	0.020571	0.000007	104.294198	11.153762
3670538543.888	857.129	0.044020	0.020578	118.890517	49.066279	0.020572	0.000008	104.294198	11.153762
3670538553.885	867.126	0.044039	0.020576	118.997023	49.342917	0.020578	0.000007	104.329700	11.245975
3670538563.889	877.130	0.044043	0.020581	118.991951	49.329743	0.020583	0.000008	104.349987	11.298668
3670538573.885	887.126	0.044057	0.020587	119.032525	49.435129	0.020586	0.000008	104.365202	11.338187
3670538583.888	897.129	0.044072	0.020585	119.118743	49.659074	0.020583	0.000008	104.349987	11.298668
3670538593.888	907.129	0.044085	0.020590	119.159317	49.764460	0.020588	0.000007	104.380417	11.377707
3670538603.889	917.130	0.044095	0.020591	119.204962	49.883019	0.020591	0.000008	104.390561	11.404053
3670538613.888	927.129	0.044103	0.020592	119.240464	49.975231	0.020596	0.000006	104.426062	11.496266
3670538623.887	937.128	0.044115	0.020594	119.291181	50.106963	0.020594	0.000007	104.410847	11.456746
3670538633.888	947.129	0.044124	0.020597	119.321611	50.186003	0.020598	0.000006	104.436206	11.522612
3670538643.887	957.128	0.044134	0.020605	119.331754	50.212349	0.020594	0.000008	104.405776	11.443573
3670538653.890	967.131	0.044145	0.020606	119.382471	50.344081	0.020603	0.000006	104.461564	11.588478
3670538663.887	977.128	0.044150	0.020609	119.392615	50.370428	0.020604	0.000006	104.466636	11.601652

3670538673.888	987.129	0.044166	0.020606	119.488977	50.620719	0.020609	0.000007	104.486923	11.654345
3670538683.888	997.129	0.044167	0.020610	119.473762	50.581199	0.020611	0.000007	104.497066	11.680691
3670538693.888	1007.129	0.044183	0.020613	119.539694	50.752451	0.020613	0.000006	104.512281	11.720211
3670538703.889	1017.130	0.044195	0.020616	119.585339	50.871010	0.020622	0.000006	104.557926	11.838770
3670538713.887	1027.128	0.044202	0.020627	119.565052	50.818317	0.020621	0.000007	104.547783	11.812423
3670538723.888	1037.129	0.044218	0.020624	119.661414	51.068608	0.020619	0.000006	104.542711	11.799250
3670538733.887	1047.128	0.044210	0.020619	119.646199	51.029088	0.020618	0.000006	104.537640	11.786077
3670538743.886	1057.127	0.044220	0.020618	119.701988	51.173994	0.020618	0.000007	104.532568	11.772903
3670538753.888	1067.129	0.044236	0.020620	119.772991	51.358419	0.020617	0.000006	104.532568	11.772903
3670538763.888	1077.129	0.044234	0.020620	119.762848	51.332072	0.020623	0.000007	104.557926	11.838770
3670538773.886	1087.127	0.044242	0.020617	119.818636	51.476978	0.020620	0.000007	104.542711	11.799250
3670538783.887	1097.128	0.044256	0.020621	119.869353	51.608710	0.020624	0.000008	104.557926	11.838770
3670538793.887	1107.128	0.044270	0.020629	119.899783	51.687749	0.020622	0.000007	104.552855	11.825596
3670538803.887	1117.128	0.044274	0.020634	119.894712	51.674576	0.020631	0.000006	104.603571	11.957329
3670538813.888	1127.129	0.044278	0.020637	119.899783	51.687749	0.020632	0.000007	104.603571	11.957329
3670538823.889	1137.130	0.044289	0.020636	119.960644	51.845828	0.020633	0.000007	104.608643	11.970502
3670538833.888	1147.129	0.044297	0.020642	119.970787	51.872174	0.020639	0.000007	104.639073	12.049541

3670538843.889	1157.130	0.044307	0.020640	120.031647	52.030253	0.020640	0.000008	104.639073	12.049541
3670538853.889	1167.130	0.044310	0.020652	119.986002	51.911694	0.020646	0.000008	104.669503	12.128580
3670538863.888	1177.129	0.044325	0.020654	120.051934	52.082946	0.020650	0.000007	104.694862	12.194446
3670538873.887	1187.128	0.044338	0.020660	120.087436	52.175158	0.020663	0.000009	104.750650	12.339352
3670538883.887	1197.128	0.044349	0.020657	120.158440	52.359583	0.020655	0.000008	104.715149	12.247139
3670538893.888	1207.129	0.044346	0.020658	120.138153	52.306890	0.020656	0.000007	104.725292	12.273486
3670538903.887	1217.128	0.044347	0.020654	120.163511	52.372756	0.020657	0.000007	104.730364	12.286659
3670538913.888	1227.129	0.044357	0.020658	120.193941	52.451796	0.020654	0.000008	104.710077	12.233966
3670538923.887	1237.128	0.044359	0.020653	120.229443	52.544008	0.020656	0.000006	104.730364	12.286659
3670538933.889	1247.130	0.044372	0.020665	120.234515	52.557181	0.020660	0.000008	104.740507	12.313005
3670538943.886	1257.127	0.044379	0.020662	120.285232	52.688914	0.020655	0.000007	104.720220	12.260313
3670538953.885	1267.126	0.044380	0.020659	120.305519	52.741607	0.020665	0.000008	104.765866	12.378871
3670538963.888	1277.129	0.044387	0.020664	120.315662	52.767953	0.020663	0.000008	104.755722	12.352525
3670538973.889	1287.130	0.044391	0.020661	120.351164	52.860165	0.020663	0.000007	104.760794	12.365698
3670538983.889	1297.130	0.044406	0.020668	120.391737	52.965551	0.020668	0.000008	104.781081	12.418391
3670538993.890	1307.131	0.044408	0.020673	120.376522	52.926032	0.020669	0.000007	104.791224	12.444738
3670539003.888	1317.129	0.044411	0.020666	120.427239	53.057764	0.020671	0.000008	104.796296	12.457911

3670539013.888	1327.129	0.044418	0.020672	120.432311	53.070937	0.020669	0.000007	104.791224	12.444738
3670539023.888	1337.129	0.044426	0.020676	120.452597	53.123630	0.020672	0.000008	104.801367	12.471084
3670539033.889	1347.130	0.044421	0.020674	120.437382	53.084110	0.020674	0.000007	104.816582	12.510604
3670539043.889	1357.130	0.044431	0.020676	120.477956	53.189496	0.020675	0.000008	104.816582	12.510604
3670539053.887	1367.128	0.044443	0.020679	120.523601	53.308055	0.020678	0.000009	104.826726	12.536950
3670539063.887	1377.128	0.044444	0.020679	120.528673	53.321228	0.020677	0.000008	104.826726	12.536950
3670539073.884	1387.125	0.044451	0.020683	120.543888	53.360748	0.020676	0.000008	104.821654	12.523777
3670539083.885	1397.126	0.044449	0.020687	120.513458	53.281708	0.020684	0.000008	104.862228	12.629163
3670539093.889	1407.130	0.044457	0.020686	120.559103	53.400267	0.020682	0.000008	104.852084	12.602816
3670539103.888	1417.129	0.044457	0.020689	120.543888	53.360748	0.020685	0.000008	104.867299	12.642336
3670539113.888	1427.129	0.044464	0.020691	120.569246	53.426614	0.020687	0.000008	104.877443	12.668682
3670539123.887	1437.128	0.044468	0.020685	120.619963	53.558346	0.020686	0.000008	104.872371	12.655509
3670539133.887	1447.128	0.044472	0.020686	120.635178	53.597866	0.020688	0.000008	104.882514	12.681855
3670539143.889	1457.130	0.044477	0.020694	120.619963	53.558346	0.020686	0.000008	104.872371	12.655509
3670539153.887	1467.128	0.044482	0.020688	120.675752	53.703251	0.020689	0.000008	104.887586	12.695029
3670539163.888	1477.129	0.044485	0.020691	120.675752	53.703251	0.020695	0.000009	104.912944	12.760895
3670539173.888	1487.129	0.044483	0.020696	120.640250	53.611039	0.020690	0.000008	104.892658	12.708202

3670539183.889	1497.130	0.044488	0.020693	120.680823	53.716425	0.020692	0.000008	104.902801	12.734548
3670539193.888	1507.129	0.044490	0.020694	120.685895	53.729598	0.020689	0.000007	104.892658	12.708202
3670539203.886	1517.127	0.044502	0.020693	120.751827	53.900850	0.020691	0.000007	104.902801	12.734548
3670539213.888	1527.129	0.044501	0.020691	120.756899	53.914023	0.020694	0.000009	104.907873	12.747722
3670539223.888	1537.129	0.044504	0.020696	120.746755	53.887676	0.020695	0.000008	104.918016	12.774068
3670539233.889	1547.130	0.044509	0.020695	120.777186	53.966716	0.020697	0.000008	104.928160	12.800414
3670539243.885	1557.126	0.044514	0.020699	120.782257	53.979889	0.020693	0.000008	104.907873	12.747722
3670539253.884	1567.125	0.044512	0.020697	120.782257	53.979889	0.020698	0.000008	104.933231	12.813588
3670539263.888	1577.129	0.044521	0.020700	120.812687	54.058928	0.020699	0.000008	104.938303	12.826761
3670539273.888	1587.129	0.044524	0.020704	120.807616	54.045755	0.020697	0.000009	104.923088	12.787241
3670539283.886	1597.127	0.044530	0.020710	120.807616	54.045755	0.020702	0.000009	104.948446	12.853107
3670539293.887	1607.128	0.044532	0.020707	120.832974	54.111621	0.020702	0.000008	104.953518	12.866280
3670539303.887	1617.128	0.044546	0.020712	120.878619	54.230180	0.020706	0.000008	104.973805	12.918973
3670539313.886	1627.127	0.044541	0.020709	120.868476	54.203834	0.020706	0.000008	104.973805	12.918973
3670539323.888	1637.129	0.044540	0.020708	120.868476	54.203834	0.020707	0.000008	104.978876	12.932147
3670539333.888	1647.129	0.044550	0.020712	120.898906	54.282873	0.020709	0.000008	104.989020	12.958493
3670539343.887	1657.128	0.044550	0.020709	120.914121	54.322392	0.020709	0.000007	104.994091	12.971666

3670539353.885	1667.126	0.044556	0.020706	120.959766	54.440951	0.020709	0.000008	104.989020	12.958493
3670539363.888	1677.129	0.044559	0.020714	120.934408	54.375085	0.020707	0.000008	104.978876	12.932147
3670539373.886	1687.127	0.044555	0.020712	120.924264	54.348739	0.020708	0.000007	104.989020	12.958493
3670539383.888	1697.129	0.044555	0.020713	120.919193	54.335566	0.020712	0.000008	105.004235	12.998013
3670539393.886	1707.127	0.044555	0.020716	120.903978	54.296046	0.020714	0.000008	105.014378	13.024359
3670539403.889	1717.130	0.044570	0.020717	120.974981	54.480471	0.020707	0.000008	104.978876	12.932147
3670539413.885	1727.126	0.044575	0.020717	121.000340	54.546337	0.020717	0.000007	105.034665	13.077052
3670539423.886	1737.127	0.044576	0.020718	121.000340	54.546337	0.020717	0.000009	105.024522	13.050705
3670539433.887	1747.128	0.044585	0.020722	121.025698	54.612203	0.020723	0.000007	105.065095	13.156091
3670539443.888	1757.129	0.044589	0.020725	121.030770	54.625376	0.020720	0.000007	105.049880	13.116572
3670539453.887	1767.128	0.044592	0.020722	121.061200	54.704416	0.020721	0.000009	105.044808	13.103398
3670539463.887	1777.128	0.044595	0.020726	121.056128	54.691243	0.020720	0.000009	105.039737	13.090225
3670539473.889	1787.130	0.044597	0.020722	121.086559	54.770282	0.020724	0.000008	105.065095	13.156091
3670539483.884	1797.125	0.044604	0.020727	121.096702	54.796628	0.020722	0.000008	105.054952	13.129745